Food & Function

ROYAL SOCIETY OF CHEMISTRY

PAPER

View Article Online
View Journal

Cite this: DOI: 10.1039/d6fo00358c

Lactobacillus reuteri BNCC186563 ameliorates lipid metabolism disorder in obese mice by activating the PPARα signaling pathway

Aibei Zhu,†[a] Wenjuan Shen,†[a] Bibi Zainab,[a] Xiaohu Luo,[a] Xiping Wu[b] and Yanan Liu *[a,c,d]

Obesity is a chronic disease that is now recognized as a global epidemic. Therefore, the need for effective therapeutic options to combat obesity cannot be overemphasized. Here, we demonstrate a novel protective role of *Lactobacillus reuteri* (*L. reuteri*) in obese mice. By using a mouse model of hyperlipidemia, we found that *L. reuteri* modulates lipid metabolism disorders in mice in a dose-dependent manner. Mechanistically, oral administration of *L. reuteri* alters the hepatic glycerophospholipid metabolic profiles of mice, thereby preventing lipid overaccumulation. In addition, *L. reuteri* activates hepatic PPARα signaling and promotes fatty acid oxidation for lipid lowering. To further confirm the critical role of the PPARα signaling pathway in obesity, we performed PPARα antagonist treatment experiments. The primary goal was to evaluate how *L. reuteri* intervention impacts the composition, functionality, and variety of liver metabolites in signaling pathways. The results showed that the PPARα antagonist GW6471 significantly reversed the weight loss effect of *L. reuteri* while altering the glycerophospholipid metabolic profile. Overall, *L. reuteri* ameliorates obesity in mice by modulating the PPARα pathway and glycerophospholipid metabolism, which may provide new ideas and avenues for promoting civic health.

Received 23rd January 2026,
Accepted 2nd April 2026

DOI: 10.1039/d6fo00358c

rsc.li/food-function

1. Introduction

Obesity is a chronic disease that is now recognised as a global epidemic.[1–3] In 2021, obesity was reported to cause an additional 2.8 million deaths from non-communicable diseases.[4–6] Current treatments for obesity include surgery, medications, reliance on dietary control, and increased exercise.[7,8] However, traditional treatments tend to have drawbacks such as being expensive, creating dependence, being ineffective, and risky.[9] Therefore, it is crucial to find effective and safe approaches to prevent obesity for improving people's health and well-being.

In recent years, probiotics have become a research hotspot because of their ability to maintain intestinal microstate balance and intestinal function, improve liver function, lower serum cholesterol, and enhance immune function and antitumor effects.[10–12] *Lactobacillus reuteri* (*L. reuteri*), a type of lactic acid bacteria, has been widely used in food, fermentation for industrial purposes, and healthcare.[13,14] Earlier research indicates that *L. reuteri* mitigates acute ischemic heart damage, combats tumors, and lessens periodontitis.[15–17] These studies suggest that *L. reuteri* is a multi-target drug with potential therapeutic effects for various diseases. In our previous study, it has been shown that peptides extracted from *Chlorella proteolytica* can effectively exert lipid-lowering effects by promoting the proliferation and enrichment of *Lactobacillus* in the intestinal tract, and *L. reuteri* is the key strain exerting lipid-lowering effects.[18] Therefore, it is reasonable to hypothesize that *L. reuteri* may be a therapeutic agent for obesity, which confirms similar findings by other researchers.[19,20] Nevertheless, despite the growing body of evidence supporting the anti-obesity potential of *L. reuteri*, the underlying molecular mechanisms remain largely unexplored. In particular, whether *L. reuteri* exerts its lipid-lowering effects through the regulation of hepatic glycerophospholipid metabolism – a criti-

[a]*Department of Food Science and Engineering, Zhejiang-Malaysia Joint Research Laboratory for Agricultural Product Processing and Nutrition, Key Laboratory for Food Microbiology and Nutrition of Zhejiang Province, Ningbo University, Ningbo 315211, China*
[b]*Department of Neurology, The Affiliated Lihuili Hospital of Ningbo University, Ningbo, 315000, PR China*
[c]*Key Laboratory of Detection and Risk Prevention of Key Hazardous Materials in Food, China General Chamber of Commerce, Ningbo Key Laboratory of Detection, Control, and Early Warning of Key Hazardous Materials in Food, Ningbo Academy of Product and Food Quality Inspection (Ningbo Fibre Inspection Institute), Ningbo 315048, China*
[d]*College of Food Science and Technology, Nanjing Agricultural University, Nanjing, 210095, PR China*
†These authors contributed equally to this work.

cal pathway involved in membrane integrity, lipid storage, and energy homeostasis – has not been systematically investigated.[21,22] Furthermore, although the peroxisome proliferator-activated receptor alpha (PPARα) signaling pathway is known to play a central role in hepatic fatty acid oxidation and lipid homeostasis,[26,29] its potential involvement in mediating the metabolic benefits of *L. reuteri* remains poorly defined. To date, no study has comprehensively examined whether *L. reuteri* modulates obesity *via* synergistic regulation of glycerophospholipid metabolism and PPARα activation. Therefore, elucidating these mechanisms is essential for understanding how *L. reuteri* improves host metabolism and for identifying novel targets for probiotic-based interventions against obesity.

The metabolic balance of lipids in the liver is crucial in the progression of obesity and associated diseases.[21] Obesity is associated with hepatic steatosis, also known as disordered hepatic lipid metabolism.[22] Significantly, hepatic lipid metabolism is regulated by a variety of signalling pathways as well as lipid metabolism-related enzymes, and the relevant signalling pathways can influence the levels of proteases associated with lipid synthesis, transport, catabolism, and oxidation by regulating the expression of transcription factors in the liver, which can lead to hepatic lipid accumulation.[23–25] Peroxisome proliferator-activated receptor α (PPARα) is one of the most widely studied regulatory pathways in lipid metabolism and is mainly expressed in cardiomyocytes, hepatocytes, renal proximal tubule cells, and intestinal epithelial cells.[26] Previous studies have shown that in non-diabetic animals with cardiac hypertrophy, low expression of PPARα will cause a decrease in myocardial fatty acid oxidation (FAO) and cardiac dysfunction.[27] In addition, PPARα controls the expression of uncoupling proteins (UCPs), such as increased levels of brown adipose tissue UCP1, hepatocyte UCP2, and skeletal muscle cell UCP3 mRNA, whose activation enhances energy and glucose homeostasis in the organism.[28] Earlier investigations have shown that activators of PPARα can prevent the onset of obesity in rodents by inhibiting adipocyte hypertrophy and hyperplasia, decreasing circulating triglyceride levels, and promoting hepatic fatty acid oxidation.[29] Despite these advances, a critical research gap persists: the regulatory effects of *Lactobacilli*, especially *L. reuteri*, on hepatic glycerophospholipid metabolism—a key branch of hepatic lipid homeostasis whose dysregulation is closely linked to hepatic steatosis and obesity—and the specific mechanisms by which *L. reuteri* modulates the PPARα signalling pathway to mediate hepatic lipid catabolism and anti-obesity effects remain largely uncharacterized. With this in view, many scientists have conducted studies on treating obesity without side effects by investigating the mechanisms of lipid metabolism.[29–31] In this regard, special attention should be paid to the prevention and treatment of probiotics.

Considering the potential interaction of lipid metabolism with *Lactobacillus reuteri* , we hypothesised that the benefits of *L. reuteri* on obesity-associated metabolic dysfunction would be mediated primarily through the modulation of lipid metabolism. We orally administered *L. reuteri* to high-fat diet-induced obese (HFD) mice and assessed the contribution of balanced lipid homeostasis in the anti-obesity effects exerted by *L. reuteri* through a series of assays of blood glucose, blood lipids, and gene expression in mice. Then, untargeted metabolomics and DIA quantitative proteomics were used to elucidate its anti-obesity mechanism. We demonstrated the regulation of lipid metabolism disorders and thus the anti-obesity effect of *L. reuteri* and found that PPARα, a key signalling pathway of lipid metabolism, may be the specific molecular mechanism to exert its effect. Therefore, we validated the mechanism of mitigating the impact of *L. reuteri* in obese mice using the PPARα antagonist and found a synergistic promotion of triglyceride metabolism. The present study provides new insights into the improvement of host health by *L. reuteri* and demonstrates the role of the PPARα signalling pathway in the host health-promoting effects exerted by *L. reuteri*.

2. Methods

2.1. Animal experiments

All animal laboratory procedures were implemented in accordance with the Guidelines for the Welfare and Ethical Use of Laboratory Animals developed by the National Standardization Administration of China and approved by the Animal Ethics Committee of Ningbo University School of Medicine (Zhejiang, China) (approval no. 11805). The 110 C57BL/6J male mice, SPF grade, 6 weeks old, were purchased from Jiangsu Jicui Pharmachem Biotechnology Co. (Jiangsu, China). The mice were housed in the Experimental Animal Center of Ningbo University, with free access to water, and the bedding was changed every 3 days. The mice were randomly divided into regular feeding (n = 30) and high-fat feeding (n = 80) groups. By referring to the previous method with slight modification, the body weight of the HFD group was 20% higher than that of the CD group, which was considered successful for modelling, and the subsequent experiments continued to be completed.[18]

For probiotic treatment, mice were modelled successfully and randomly assigned to the following treatment groups: control, HFD, H-*L. reuteri* (1×10^{10} CFU mL^{-1}), M-*L. reuteri* (1×10^{9} CFU mL^{-1}) and L-*L. reuteri* (1×10^{8} CFU mL^{-1}), followed by daily gavage treatment for 11 weeks. During the treatment period, the control group was given an equal volume of saline. Body weight was monitored throughout the process, and at the end of the treatment, mice were kept fasted for 12 h, anaesthetized with anhydrous ether, and blood samples were collected using the eyeball removal method. The liver, intestines and fat were harvested and stored in a refrigerator at −80 °C.[32]

For antagonist treatment, after successful modelling, mice were randomly assigned to the following treatment groups: NCD, NCD + GW6471, HFD, HFD + GW6471 (10 mg kg^{-1} GW6471), HFD + *L. reuteri* (1×10^{10} CFU mL^{-1}), and HFD + *L. reuteri* + GW6471 (1×10^{10} CFU mL^{-1} *L. reuteri* + 10 mg kg^{-1}

GW6471) by daily gavage for 11 weeks. Body weight was tested during the treatment. At the end of the treatment period, sample collection and processing were performed as described above for the probiotic treatment.

2.2. Test strains and treatments

The *L. reuteri* lyophilised powder was purchased from Bei Na Bio (Hebei, China), with the strain number BNCC186563. After dissolving with 0.5 mL of MRS medium, the bacterial solution was spread evenly onto the plate and coated evenly, and colonies appeared after about 24 h. The bacterial solution was then incubated in the MRS medium for 12–16 h at 37 °C anaerobically. The cultured bacteria were recovered by centrifugation (5000*g*, 4 °C, 5 min) and rinsed three times with sterile PBS and then resuspended. The density of bacteria was adjusted to 1×10^8 CFU mL^{-1}, 1×10^9 CFU mL^{-1}, and 1×10^{10} CFU mL^{-1} by measuring the OD_{600} of three concentration gradients.

2.3. Chemicals and reagents

The PPARα antagonist GW6471 (Selleck, Shanghai, China; Cat#S2798, Lot#S279805) was suspended in a vehicle of 0.5% carboxymethyl cellulose sodium (CMC-Na; Selleck, Cat#S6703, Lot#S670308) for daily administration.

2.4. Oral glucose tolerance test (OGTT)

The OGTT was conducted in response to previous studies with slight modifications.[33] The mice were placed on an overnight fast for 12–14 hours without water and a D-glucose solution was prepared in PBS at a concentration of 200 mg mL^{-1}. The glucose solution was injected intraperitoneally at a dose of 2 g kg^{-1} (10 μL g^{-1}) in the morning of the next day, and the changes in the glucose value of the mice were detected by taking blood from the tail vein of the mice at 0, 30, 60, 90, and 120 min, respectively.

2.5. Insulin tolerance test (ITT)

The ITT was performed in response to prior studies with mild modifications.[34] In the ITT, insulin (0.75 U kg^{-1} body weight) was given *via* an intraperitoneal injection after a 4 h fast. All ITT trials were performed at the same designated time as the OGTT.

2.6. Biochemical analysis

Serum levels of triglycerides (TG), total cholesterol (T-CHO), high-density lipoprotein cholesterol (HDL-C), low-density lipoprotein cholesterol (LDL-C), alanine aminotransferase (ALT), and aspartate aminotransferase (AST) were measured according to the instructions in the kit (Jiancheng, Nanjing, China; Cat#A110-1-1).[35]

2.7. Histopathological analysis

After the samples were fixed in 10% formalin fixative for 24 h, the tissue sections were made through the steps of washing, dehydration,clearing, paraffin infiltration, embedding, sectioning, and staining, and the thickness of the sections was about 6 μm. After H&E staining, the pathological and morphological changes of liver tissues were observed under a microscope (×20), and the corresponding tissue images were captured using an image acquisition system.[36]

Fresh frozen sections were first rewarmed and dried, fixed with a fixative solution, and then stained with oil red for 8–10 min after water evaporation, taking care to cover and avoid light during the staining process. The staining effect was examined under a microscope (×20), and the corresponding tissue images were captured using an image acquisition system.[37]

2.8. Enzyme-linked immunosorbent assay (ELISA)

Serum carnitine palmitoyltransferase (CPT-1), fatty acid synthase (FAS), and acetyl coenzyme A carboxylase (ACC) were all measured according to the manufacturer's protocols using mouse-specific commercial ELISA kits (Shanghai Ruifan Biological Technology Co., Ltd, Cat#RXFP3).[38] Total RNA was extracted from the liver.

2.9. RNA extraction and quantification

Total RNA was extracted from 50 mg liver samples using a lysate according to the Animal RNA Rapid Extraction Kit (Sangon Biotech, Shanghai, China; Cat#B518621-0050), and reverse transcription was performed using the HiScript II Q RT SuperMix for qPCR (+g DNA wiper) kit (Vazyme, Nanjing, China; Cat#DM601-01). Real-time PCR was performed using the Taq Pro Universal SYBR qPCR Master Mix kit (Vazyme, Nanjing, China; Cat#QN213-01). In addition, the expression levels of the target genes were expressed as mean ± SEM, and the expression of the internal reference GAPDH was normalised using the ΔΔCt method.[39]

2.10. Untargeted metabolomics study

The liver samples weighed 50 mg, and 1000 μL of extraction solution (methanol : acetonitrile : water = 2 : 2 : 1 (v/v), containing 1 μg mL^{-1} of the internal standard) was added and vortexed to mix for 30 s.[40] The samples were then extracted and mixed for 30 s. Milling treatment was performed for 4 min, and ultrasonic treatment was performed for 5 min (in an ice-water bath) and repeated three times. The samples were centrifuged (Centrifuge 5424 R, Eppendorf, Germany) at 4 °C and 12000 rpm (Thermo Fisher Scientific, USA) for 15 min, and the supernatant was taken in the injection bottle for testing.

The target compounds were separated on a Waters ACQUITY UPLC HSS T3 column (2.1 mm × 100 mm, 1.8 μm; Waters, USA) using a Vanquish Flex UHPLC system (Thermo Fisher Scientific, USA). The A phase of the liquid chromatography was an aqueous phase containing 0.1% formic acid in positive ion mode and 5 mmol L^{-1} ammonium acetate in negative ion mode; the B phase was acetonitrile. The gradient elution was used: 0–1.0 min, 1% B; 1.0–8.0 min, 1%–99% B; 8.0–10.0 min, 99% B; 10.0–10.1 min, 99%–1% B; and 10.1–12 min, 1% B. The flow rate of the mobile phase was 0.5 mL min^{-1}, the column temperature was 35 °C, the temperature of the sample tray was 4 °C, and the injection volume was 2 μL.

2.11. Non-labelled quantitative proteome

The liver samples to be tested were ultrasonically broken by adding 3× protein lysate and 1 : 50 protease inhibitor for 180 s, boiling water bath for 3 min, centrifuged for 20 min to remove the supernatant, and dispensed as described previously[41]—the fluorescence method with tryptophan as the standard curve determined the total protein concentration. The peptides were extracted by the filter-aided sample preparation (FASP) method, and the enzymatically cleaved peptides were desalted by SOLAμHRP, concentrated, lyophilised, and re-solubilised using 0.1% FA.

The mass spectrometry data were acquired using data-independent acquisition (DIA) mode scanning. DIA method: primary mass spectrometry resolution of 60 000, maximum injection time of 50 ms, target Automatic Gain Control (AGC) of 400 000, scanning range of 400–1500. The scanning resolution was set to 30 000, the range was set to Auto, the maximum ion injection time was 100 ms, the target AGC was set to 100 000, the normalised fragmentation energy was 31%, and RF was 40%. Normalised fragmentation energy was 31% and RF was 40%.

2.12. Statistical analysis

The obtained data were expressed as mean ± SEM and displayed using the GraphPad Prism 9.0 programme (GraphPad Software, San Diego, Canada). When comparing two groups, a two-tailed Student's t-test was used to determine statistical significance. When more than two groups were investigated, comparisons between groups were made using Tukey-corrected one-way ANOVA.

3. Results

3.1. *L. reuteri* attenuates weight gain in obese mice

Different diets were given to the control, HFD, H-*L. reuteri*, M-*L. reuteri*, and L-*L. reuteri* groups for 11 weeks (Fig. 1A). The results showed that *L. reuteri* effectively inhibited HFD-induced weight gain from week 2 onwards (Fig. 1B and C). In addition, HFD feed for 11 weeks significantly increased liver weight and epididymal fat weight compared to control CD feeding. In contrast, under the intervention of 3 doses of *L. reuteri* in high, medium, and low doses, HFD-fed mice showed different degrees of reduction in liver and epididymal fat, indicating that *L. reuteri* mitigated obesity (Fig. 1D).

A high-fat diet (HFD) leads to excess energy in the body, resulting in a homeostatic imbalance between blood glucose and insulin.[42–44] To clarify the effect of *L. reuteri* on blood glucose, we performed an OGTT and ITT. The blood glucose levels of mice in the HFD group were elevated compared to the control group during the 0–120 min period following glucose injection, with the peak blood glucose observed at 30 min. The highest blood glucose value also appeared at 30 min in all administered groups, with the Area Under the Curve (AUC) of OGTT in the H-*L. reuteri* group; the AUC of the OGTT was considerably lower in comparison with the model group (Fig. 1E and F). The blood glucose of mice in each group decreased the most at 0–30 min after insulin injection, in which the AUC of the H-*L. reuteri*, M-*L. reuteri*, and L-*L. reuteri* groups were significantly smaller than that of the HFD group (Fig. 1E and F). To sum up, it is evident that *L. reuteri* enhances glucose tolerance and insulin responsiveness in obese mice, with the most significant impact noted in the H-*L. reuteri* group. These data indicate that daily treatment with *L. reuteri* modulates host metabolic homeostasis. In short, *L. reuteri* has preventive and therapeutic effects on obesity by reducing weight gain and organ weight and improving glucose homeostasis.

3.2. *L. reuteri* ameliorates lipid metabolism disorders in obese mice

Previous research has indicated that *L. reuteri* is instrumental in both preventing and treating obesity through its regulation of blood glucose balance.[45] In the meantime, lipid metabolism disorders have long been recognised as an essential factor contributing to obesity in the host.[46] Therefore, we conducted a series of assays. Changes in serum lipid levels in mice disclosed that TG and LDL-C levels in the sera of mice in the high-fibre food group were conspicuously hiked as opposed to the control group. The *L. reuteri* high, medium, and low dosage groups were able to show varying degrees of reduction in TC, TG, and LDL-C levels, with the lipid levels in the H-*L. reuteri* group being much closer to those of the control group (Fig. 2A and B). Furthermore, the HFD group showed a marked decrease in HDL-C levels relative to the control group. In contrast, *L. reuteri* high, medium, and low dose groups increased HDL-C levels to varying degrees, but there was no significant difference (Fig. 2B).

The ALT and AST levels are shown in figure2. ALT and AST levels were markedly elevated ($P < 0.0001$) in the livers of mice in the HFD group compared to those in the control group, indicating substantial liver damage. However, ALT and AST levels were highly ($P < 0.0001$) reduced in the livers of mice after intervention in the *L. reuteri* high, medium, and low dose groups (Fig. 2C). Morphological observations further confirmed this result, showing a significant reduction in hepatocellular lipid accumulation and considerable alleviation of hepatic steatosis after *L. reuteri* intervention (Fig. 2D). These results indicated that *L. reuteri* effectively ameliorated liver injury in mice caused by the high-fat diet.

3.3. *L. reuteri* alters the glycerophospholipid metabolic profile in mice

In the last part of the experiment, we concluded that *L. reuteri* ameliorated liver damage in high-fat mice. Nevertheless, it is not enough to study this, and the causes of these changes need to be explored in more depth. Therefore, we measured critical regulatory enzymes related to fatty acid production in the mouse liver to understand fat accumulation *in vivo*. As the dose levels of *L. reuteri* increased, there was a gradient of decreasing levels of the synthases – ACC and FAS, with an opposite trend for the catabolic enzyme CPT-1 (Fig. 3A–C). These data suggested that the *L. reuteri* dose had an effect on fatty acid metabolism in high-fat mice and that this effect had a dose–effect relationship.

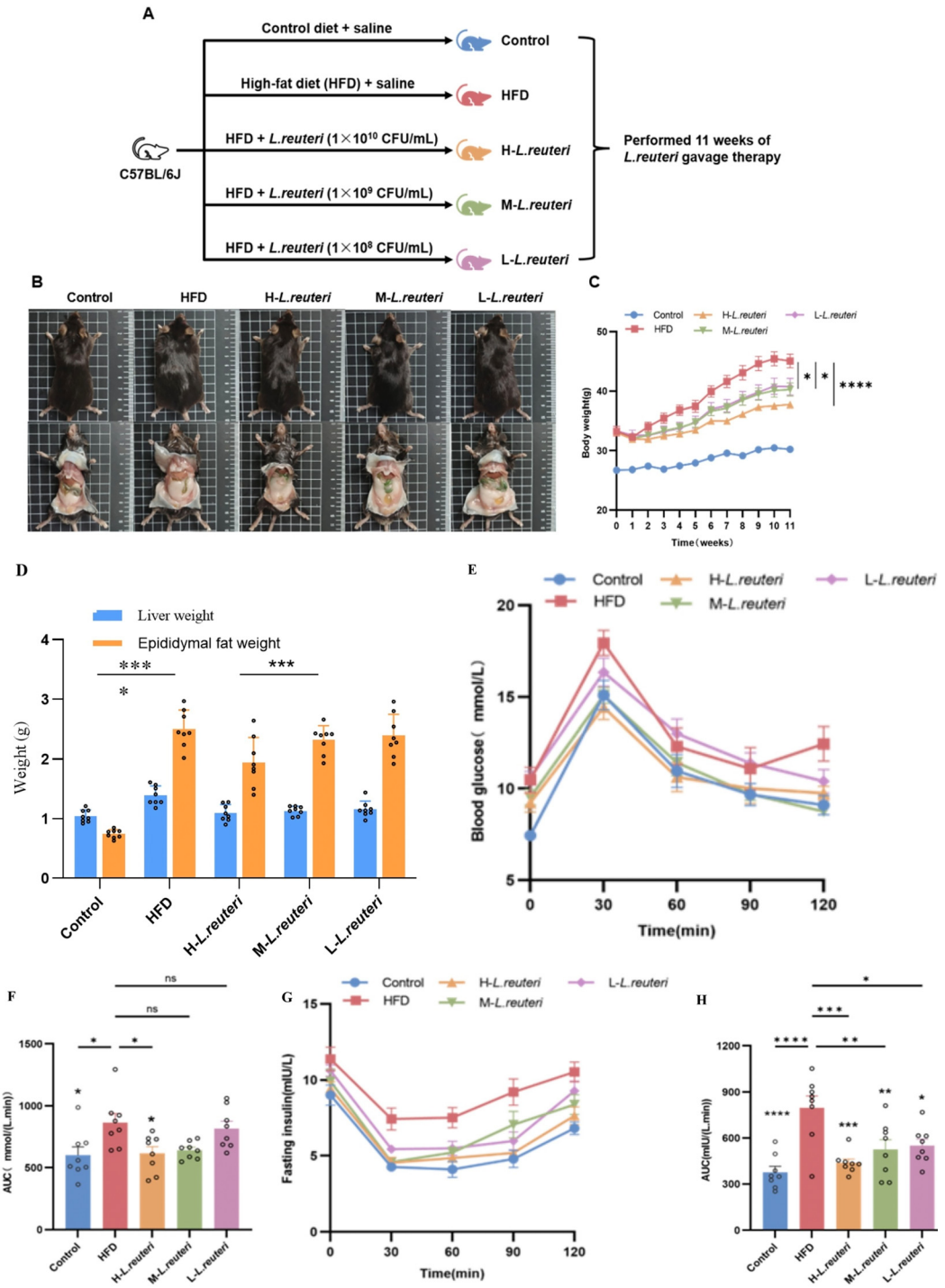

Fig. 1 *L. reuteri* alleviates weight gain in obese mice. (A) Experimental design. (B) Appearance of mice after 11 weeks of feeding. (C) 11-week body weight changes. (D) liver weight and epididymal fat weight. (E) GTT. (F) GTT AUC. (G) ITT. (H) insulin resistance AUC. Data: mean ± SEM *vs.* the HFD group. $P < 0.05$, $P < 0.01$, $^{*}P < 0.001$ and $^{**}P < 0.0001$.

The control, HFD, and H-*L. reuteri* groups with the best therapeutic effect were selected for untargeted metabolomics analysis. Partial least squares discriminant analysis (PLS-DA) showed different metabolite compositions in the control and HFD groups. After *L. reuteri* gavage, the metabolites in the HFD group changed significantly (Fig. 3D–G). The control group *vs.* the HFD group showed 76 significantly up-regulated metabolites and 37 significantly down-regulated metabolites; the HFD group *vs.* the H-*L. reuteri* group showed 45 significantly up-regulated metabolites and 80 significantly down-regulated metabolites (Fig. 4A). Then, we performed a difference analysis, listing 30 key differential metabolites (Fig. 5).

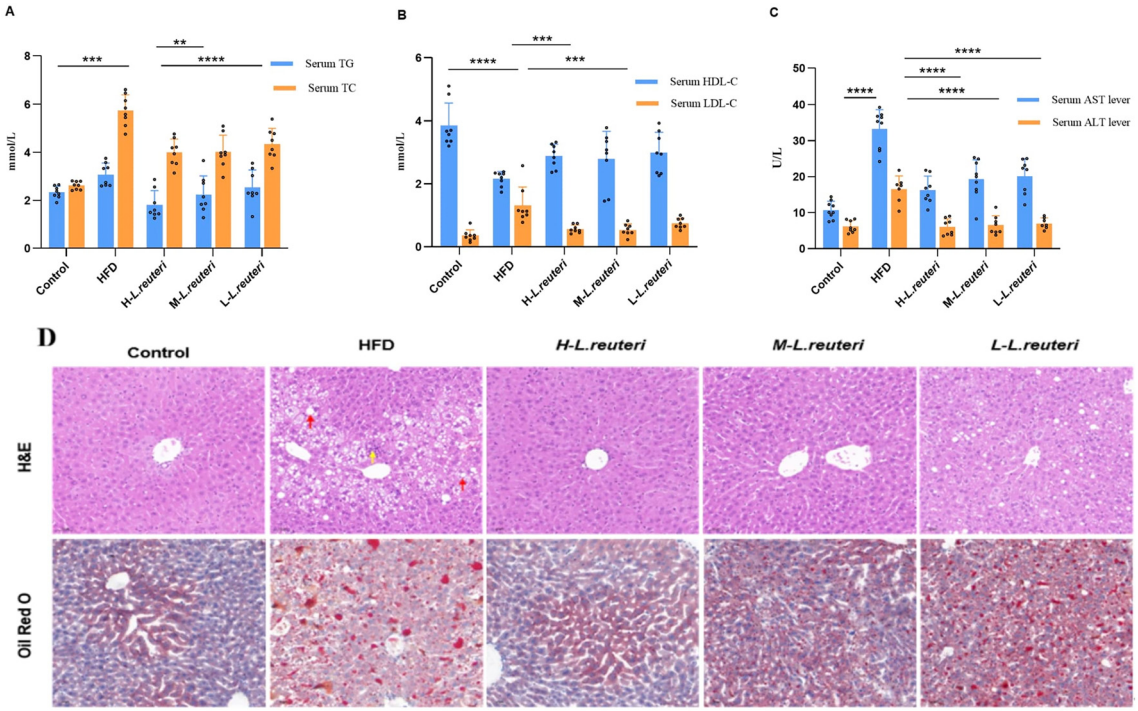

Fig. 2 *L. reuteri* ameliorates lipid metabolism disorders in obese mice. (A) The level of TG and TC in serum. (B) The level of HDL-C and LDL-C in serum. (C) The level of ALTand AST in serum. (D) Representative H&E-stained and Oil Red O-stained mouse liver sections with a scale bar representing ×20. Data are expressed as means ± SEM. **P* < 0.05, ***P* < 0.01, ****P* < 0.001 and *****P* < 0.0001 as compared to the HFD group.

Meanwhile, correlation analysis revealed that the metabolites were mostly clustered in the glycerophospholipid metabolic pathway (Fig. 4B). These key differential metabolites in glycerophospholipid metabolism play specific regulatory roles in lipid homeostasis: phosphatidylcholine (PC) acts as a core biological membrane component to maintain membrane fluidity and permeability, while also serving as a key precursor for hepatic very low-density lipoprotein (VLDL) synthesis that directly regulates peripheral lipid uptake and transport;[21,71] phosphatidylethanolamine (PE) cooperates with PC to stabilize the membrane structure, can be converted to PC *via* phosphatidylethanolamine methyltransferase (PEMT) to replenish hepatic phospholipid pools, and supports mitochondrial membrane function to ensure normal fatty acid β-oxidation;[22,71] phosphatidic acid (PA), a central intermediate in this pathway, initiates lipid droplet formation by binding perilipin proteins to promote lipid storage, while activating the mTOR pathway to couple lipid synthesis with cellular processes;[48,66] lysophosphatidylcholine (LPC), generated by phospholipase A2 (PLA2)-mediated hydrolysis of PC, acts as a ligand for lipid transfer proteins (LTPs) to mediate fatty acid transmembrane transport and activates PPARα to upregulate genes related to fatty acid oxidation.[26,28,64]

The accumulation of various metabolites was analysed using the KEGG database (Kyoto Encyclopedia of Genes and Genomes, https://www.kegg.jp/). Among the lipid metabolism-related pathways enriched in the control and H-*L. reuteri* groups compared to the HFD group, glycerophospholipid metabolism exhibited prominent changes, and the metabolites showed significant correlations with each other (Fig. 6A and B). In summary, *L. reuteri* achieves lipid-lowering effects by altering the glycerophospholipid metabolic profile.

3.4. *L. reuteri* alters the pattern of expression of proteins involved in glycerophospholipid metabolism in the livers of obese mice

Using an Astral-DIA quantitative proteomics study, we found differences between the H-*L. reuteri* and HFD groups at the proteome level. Proteomes with a multiplicity of difference – FC ≥ 1.2 and a *p*-value <0.05 were used as differential proteins. As shown, the HFD group *vs.* control group had 806 differential proteins, of which 304 were up-regulated and 502 were down-regulated in expression. The H-*L. reuteri vs.* HFD groups had 768 differential proteins, of which 509 were up-regulated and 259 were down-regulated in expression (Fig. 7A). Venn analysis was used to identify the differential proteins shared between the groups, and there were 459 differential proteins shared between the HFD group *vs.* the control group and the H-*L. reuteri* group *vs.* the HFD group, of which there was a trend of reversal after *L. reuteri* intervention (Fig. 7B). To explore the changes in triglyceride metabolism-related proteins after *L. reuteri* intervention, differential proteins related to glycerol ester metabolism were identified from the comparison between the H-*L. reuteri* and HFD groups and subjected to

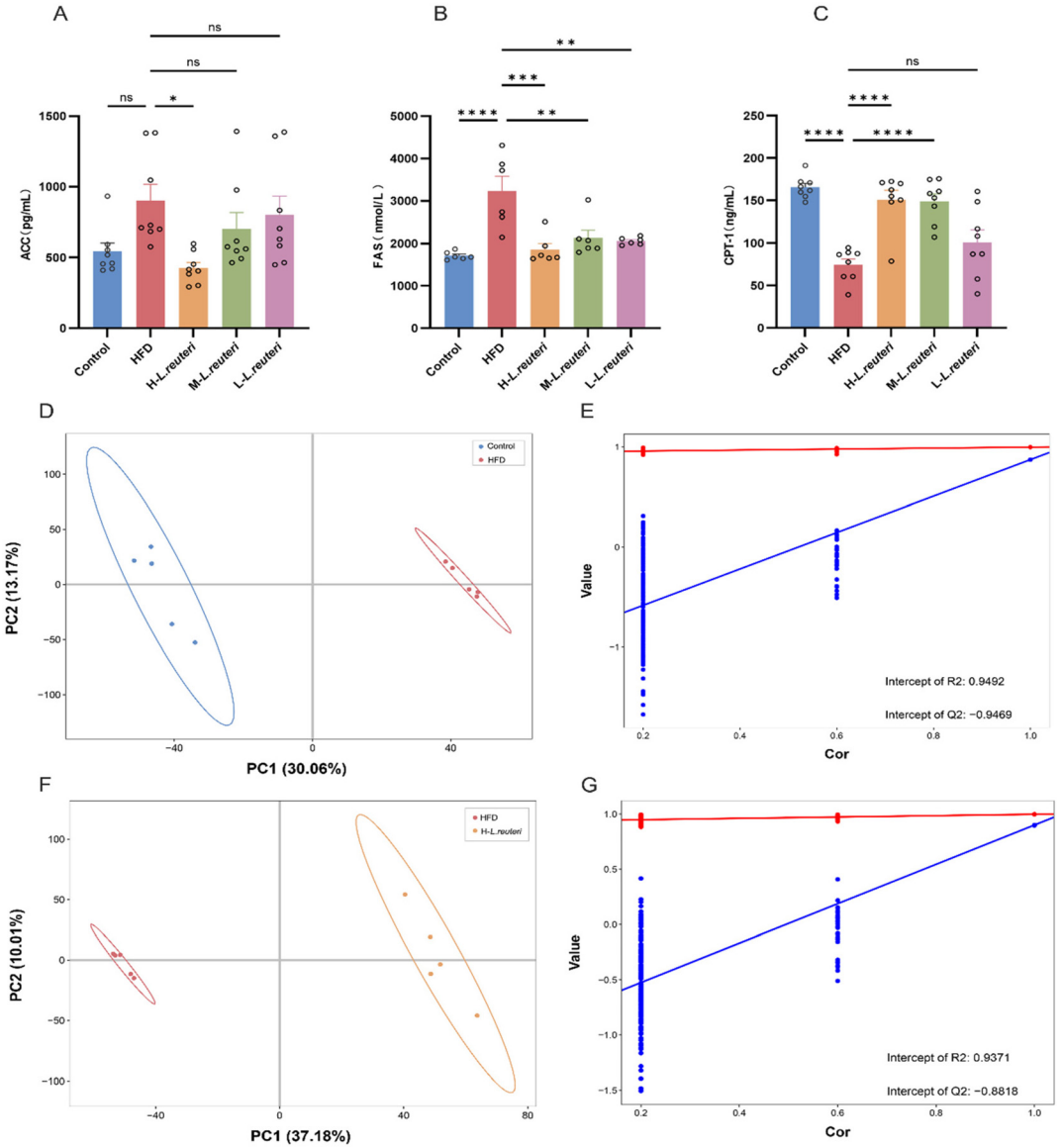

Fig. 3 *L. reuteri* modulates fatty acid metabolism in high-fat mice. (A) The level of ACC in serum. (B) The level of FAS in serum. (C) The level of CPT-1 in serum. (D) Control *vs.* HFD group comparison by PLS-DA analysis. (E) Comparison of the control and HFD groups for replacement test plots. (F) HFD *vs.* H-*L. reuteri* group comparison by PLS-DA analysis. (G) Comparison of HFD and H-*L. reuteri* groups for replacement test plots. Data are expressed as means ± SEM. **P* < 0.05, ***P* < 0.01, ****P* < 0.001 and *****P* < 0.0001.

KEGG pathway enrichment analysis (Fig. 7C). Subsequently, the pathway differential proteins were analysed. Functional annotation of the H-*L. reuteri* group with the HFD group has been identified in terms of glyceride metabolism-related proteins for KEGG pathway enrichment analysis (Fig. 8A and B). In the H-*L. reuteri* group, the levels of differential proteins Etnk1, Pcyt2, Gpat4, Etnppl, and Lpin2 were notably downregulated, whereas Agpat3, Cdipt, and Gpd2 were significantly upregulated when compared to the HFD group (Fig. 8C). These results suggest that *L. reuteri* alleviates obesity in mice in a manner that regulates differential proteins of the glyceride metabolic profile.

3.5. *L. reuteri* affects the PPARα signalling pathway

Upon further screening for essential differential proteins, the significant changes in the differential protein apolipoprotein A5 (Apoa5) in the H-*L. reuteri* group compared to the HFD group caught our attention (Fig. 9A). It has been suggested that *APOA5* may be the gene with the most substantial influence on triglyceride and metabolism.[47] There is a close relationship between triglyceride metabolism and glycerophospholipids metabolism. They both involve the glycerol molecule as a core structure, intersecting during fatty acid synthesis, storage, and transport.[48] Interestingly, APOA5 also

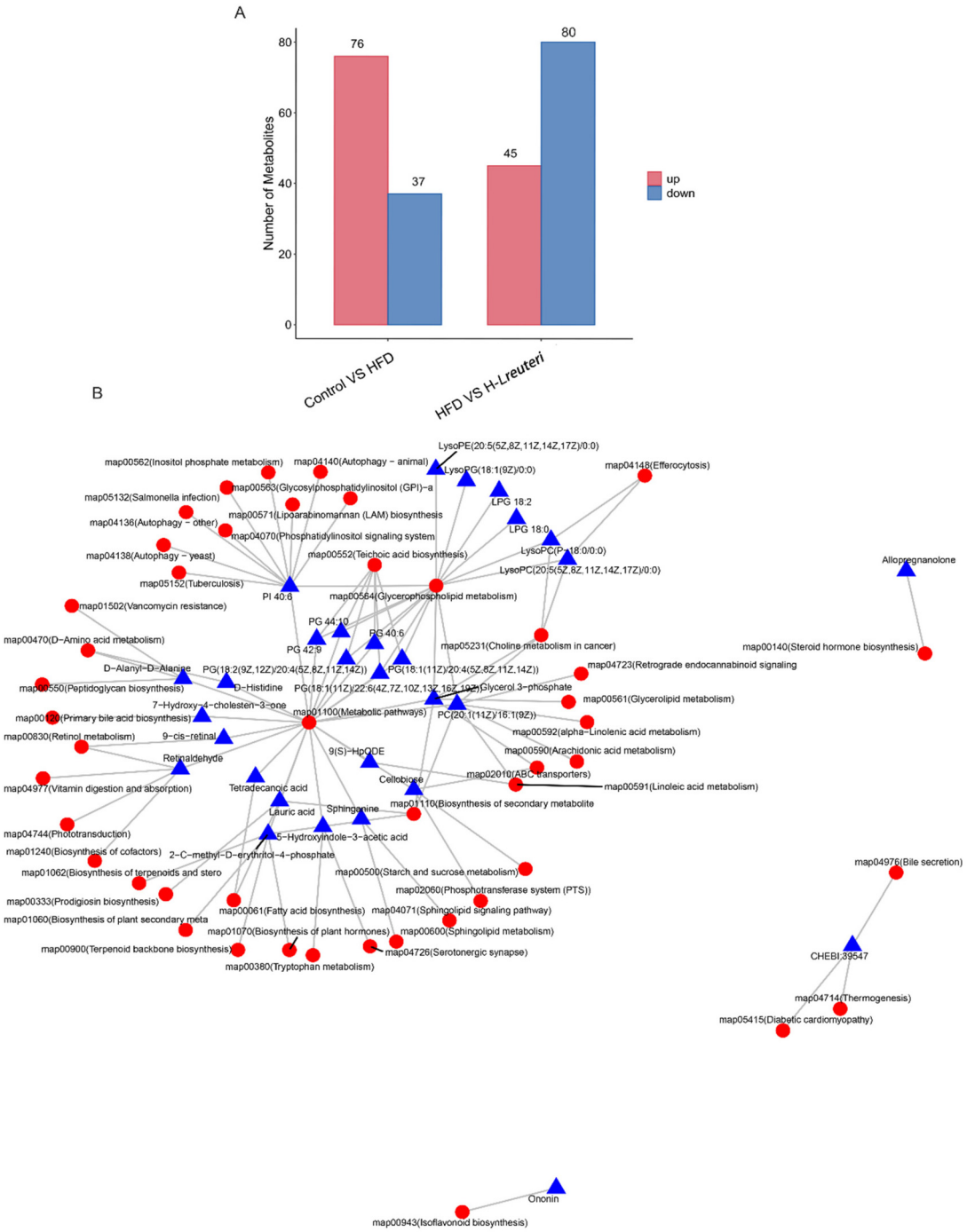

Fig. 4 *L. reuteri* alters glycerophospholipid metabolic profiles in obese mice. (A) Number of metabolites. (B) Network diagram of metabolite correlation analysis for the control, HFD and H-*L. reuteri* groups.

belongs to the PPARα signalling pathway. Therefore, we speculate whether *L. reuteri* achieves its lipid-lowering effect through the PPARα signalling pathway.

Thus, we first analysed the changes in the PPARα signalling pathway differential proteins. Compared with the HFD group, the differential proteins Apoa5 and Fabp2 were strikingly up-regulated, and Cyp4a12a, Pck1, and Slc27a4 were significantly down-regulated in the H-*L. reuteri* group (Fig. 9B). We then analyzed the changes in the lipid metabolism regulatory pathway PPARα. The mRNA expression of PPARα, adiponectin, AdipoR1 and AdipoR2 was apparently diminished and that of ApoC3 was slightly elevated in the liver tissues of mice in the HFD group compared with that in the control group. Pparα, adiponectin, AdipoR1, and AdipoR2 were utterly increased in the liver tissues of mice in the H-*L. reuteri* group compared to the HFD group, and AdipoR1 and AdipoR2 mRNA expression was sharply elevated. The mRNA

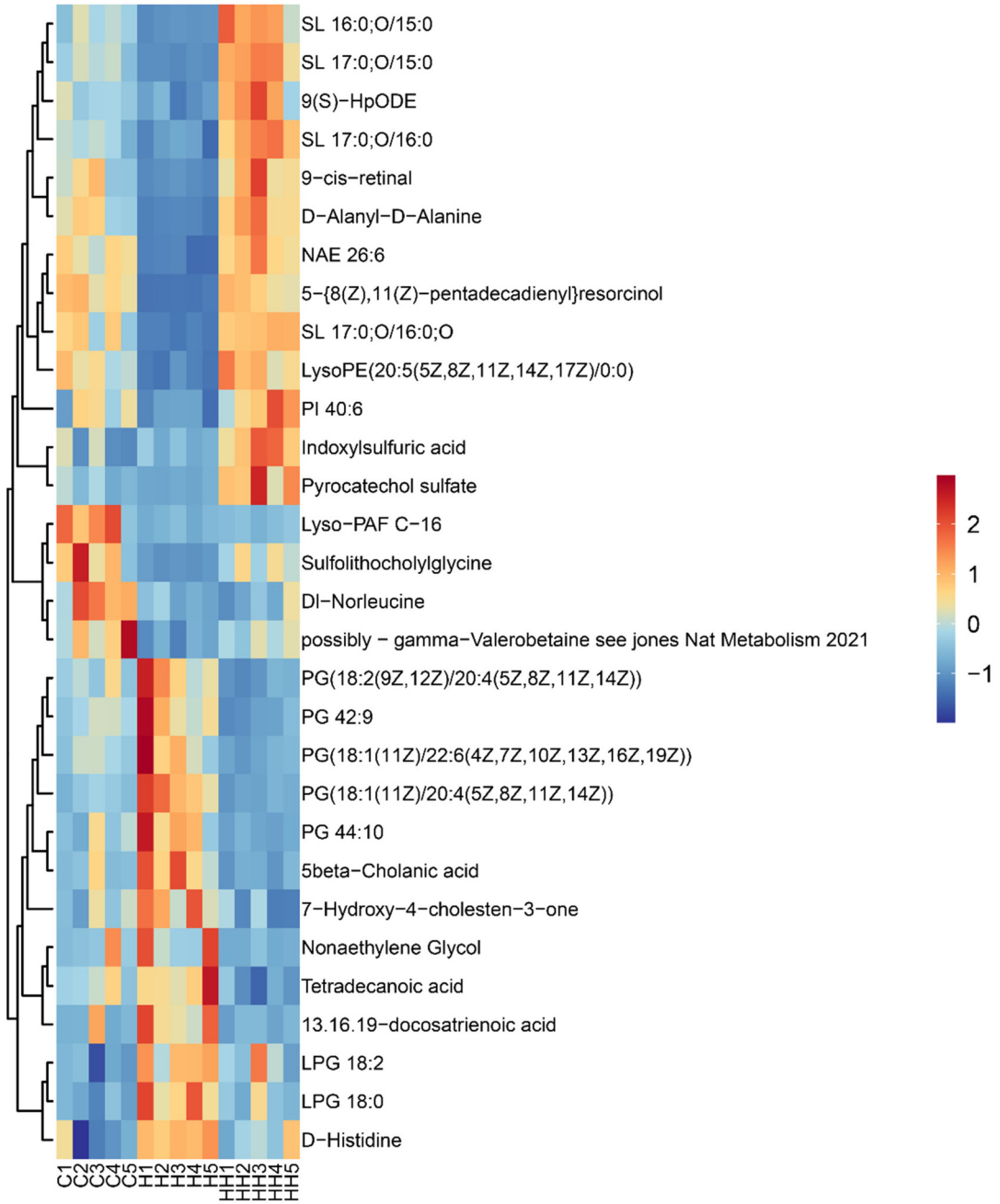

Fig. 5 *L. reuteri* alters the key differential metabolites in obese mice. Heat maps of off-target metabolites in the control, HFD and H-*L. reuteri* groups.

expression of ApoC3 showed a significant decrease. The *L. reuteri* medium and low dose groups also showed some improvement, but except for a substantial increase in the expression of PPARα, the others were not statistically significant (Fig. 9C–H). These results suggest that *L. reuteri* ultimately ameliorates obesity in mice by activating the PPARα pathway.

3.6. PPARα antagonists impair the efficacy of *L. reuteri* in ameliorating obesity in mice

To provide additional insight into the essential utility of PPARα in ameliorating obesity through *L. reuteri*, C57 mice were treated with a high-fat diet and the PPARα antagonist GW6471, respectively (Fig. 10A). The mice in the NCD + GW6471 group exhibited a pronounced gain in liver and epididymal fat weights compared to the NCD group ($P < 0.05$), but there was no major difference in the change in body weight ($P > 0.05$). The mice in the HFD + *L. reuteri* group experienced a prominent decline in liver and epididymal fat weights ($P < 0.05$) when measured in comparison with the HFD group ($P < 0.0001$), as well as a decrease in body weight ($P < 0.01$). In contrast, mice in the HFD + GW6471 group displayed a distinct increase in liver and epididymal fat weights ($P < 0.05$) and an

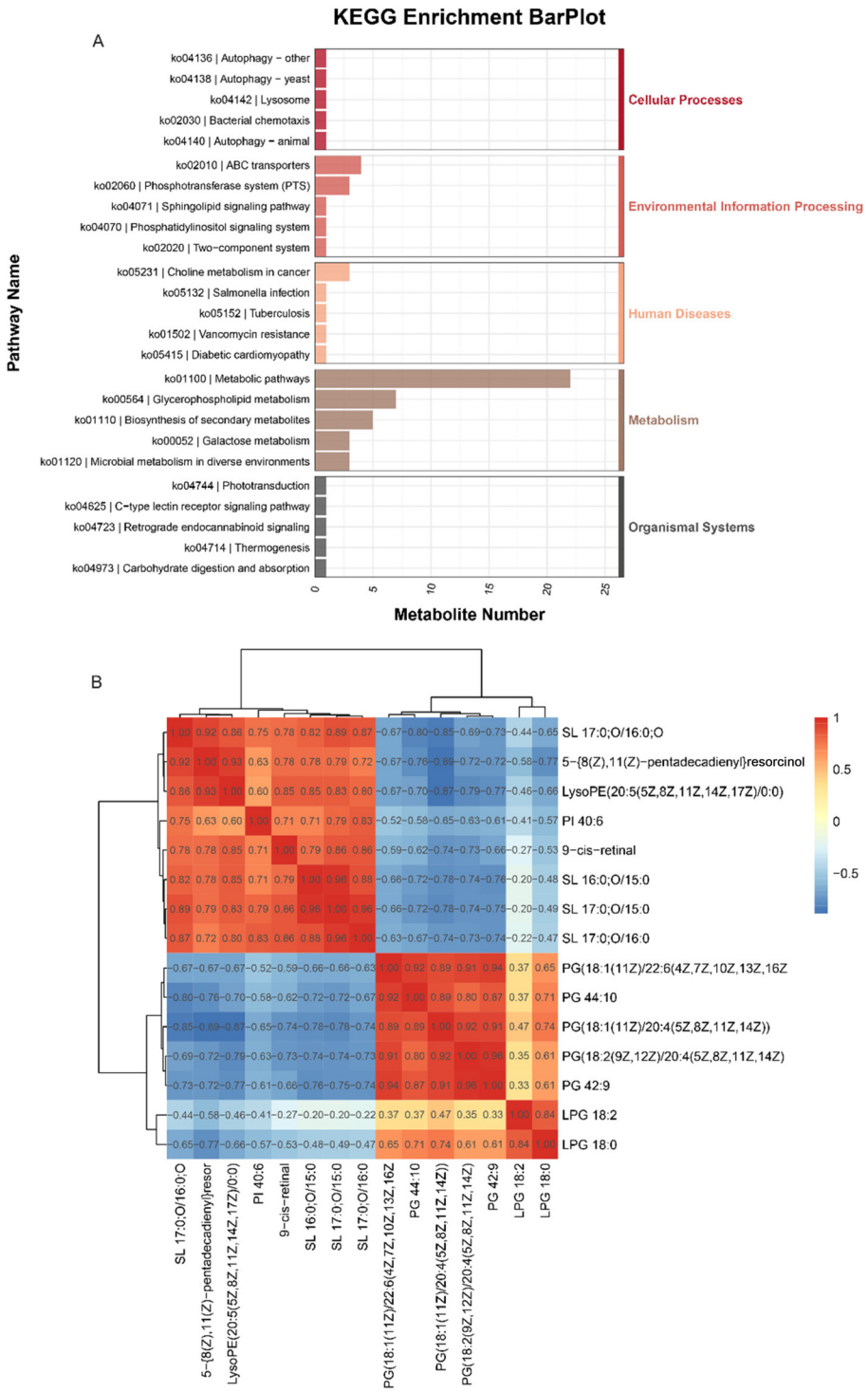

Fig. 6 Analysis of differential metabolite correlations in *L. reuteri* altered obese mice. (A) Control, HFD and H-*L. reuteri* group KEGG cascade maps. (B) Control, HFD and H-*L. reuteri* group correlation heatmaps.

increase in body weight ($P < 0.01$). In addition, mice in the HFD + GW6471 + *L. reuteri* group presented a remarkable ($P < 0.05$) increase in liver and epididymal fat weights ($P < 0.001$) and an augmentation of body weights ($P < 0.05$) as observed in the HFD + GW6471 + *L. reuteri* group as compared to the HFD + *L. reuteri* group (Fig. 10B–D and Fig. 11A and B).

TG levels were appreciably higher in the NCD + GW6471 group *versus* the NCD group ($P < 0.001$), and serum TG, TC and LDL levels were substantively higher in the HFD + *L. reuteri* and HFD + GW6471 groups *versus* the HFD group ($P < 0.0001$) ($P < 0.01$) ($P < 0.01$). Serum TG, TC and LDL levels were obviously higher in the HFD + *L. reuteri* group when com-

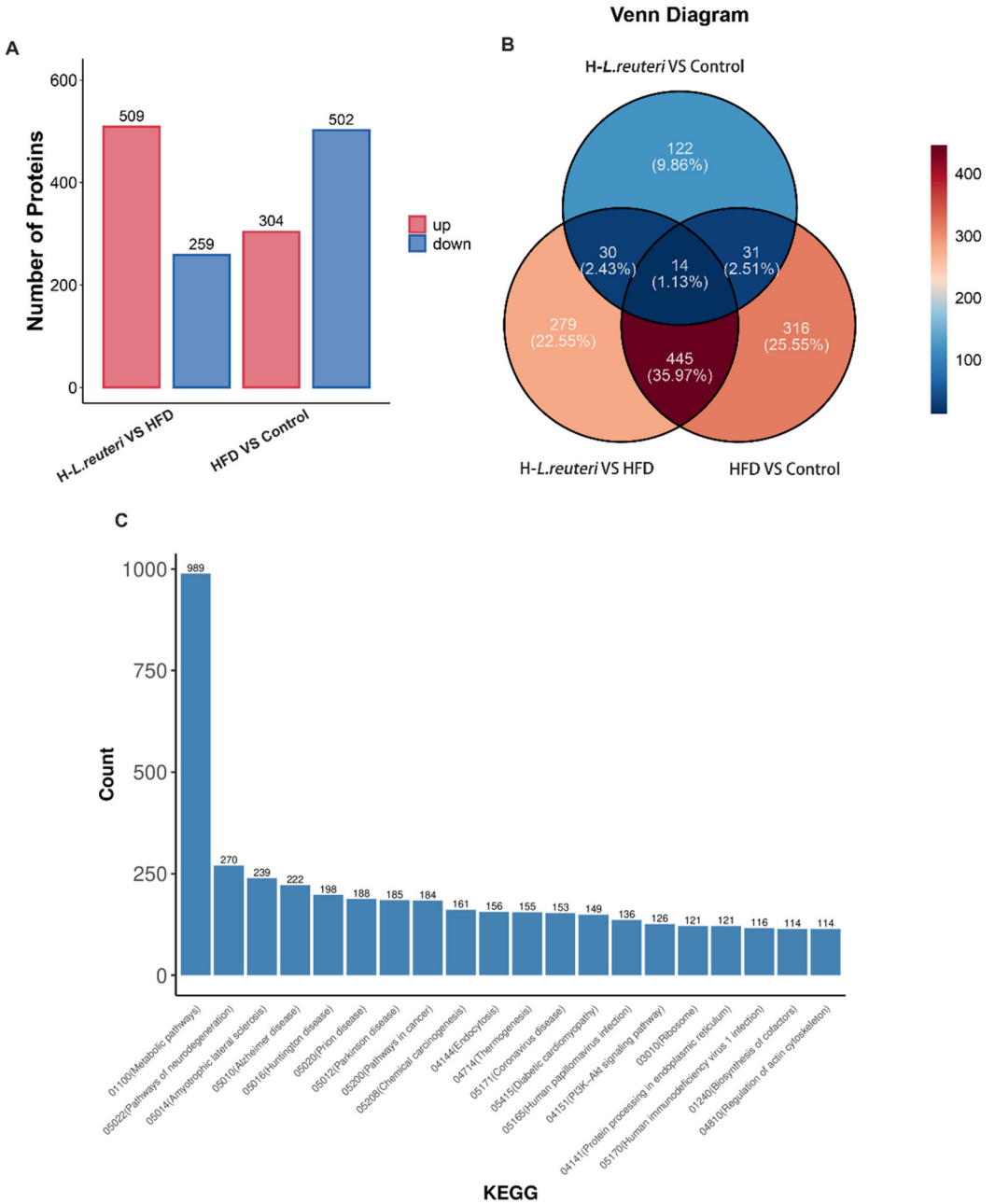

Fig. 7 *L. reuteri* protein changes after intervention in obese mice. (A) Histogram of differential protein statistics. (B) Control, HFD, and H-*L. reuteri* group Venn diagrams. (C) Protein function KEGG annotation.

pared to those in the HFD + *L. reuteri* group. Serum TG and TC levels were appreciably higher ($P < 0.05$) in the HFD + *L. reuteri* + GW6471 group compared to the HFD + *L. reuteri* + GW6471 group (Fig. 11C–E). These results indicated that *L. reuteri* exerted lipid-lowering effects, while the PPARα antagonist GW6471 significantly attenuated the weight loss effect of *L. reuteri*.

3.7. PPARα synergizes with glycerophospholipid metabolism to exert lipid-lowering effects

To investigate whether there is a potential relationship between the regulation of the PPARα signaling pathway in obese mice and glycerol ester metabolism, this study used Pearson's correlation coefficients to analyze the correlation between differential proteins of the two pathways. The closer the correlation is to 1, the higher the expression similarity of the two pathways. The results showed that six differential proteins of the PPARα signaling pathway genes Cyp4a12a, Pck1, and Apoa5 showed different degrees of strong correlation with eight differential proteins of the glycerol ester metabolism pathway genes Etnk1, Pcyt2, and Gpat4 (Fig. 12D). Based on the PPARα signaling pathway differential proteins, a joint analysis was established to correlate

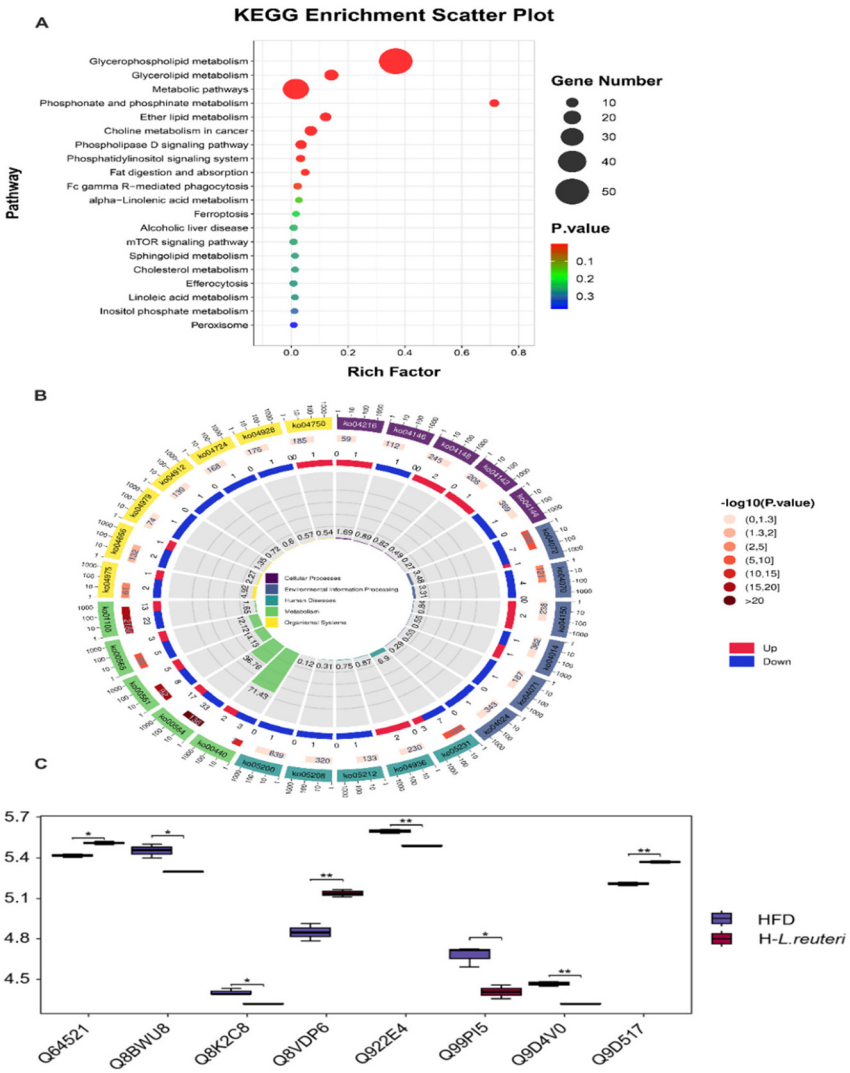

Fig. 8 Modulation of hepatic triglyceride metabolism-related protein expression by *L. reuteri* in obese mice. (A) Bubble diagram and (B) circle plot present KEGG pathway enrichment of glycerophospholipid metabolism proteins from the H-*L. reuteri vs.* HFD group comparison. (C) Box line plot shows differential proteins in glycerophospholipid metabolism, with UniProt-gene correspondences as follows: Q9D517/Agpat3, Q9D4V0/Etnk1, Q922E4/Pcyt2, Q8VDP6/Cdipt, Q8K2C8/Gpat4, Q64521/Gpd2, Q8BWU8/Etnppl and Q99PI5/Lpin2.

with glycerophospholipid-related metabolites, and the results showed that metabolites such as LPC 18 : 2, PC18:2e, and LPG 18 : 0 were positively associated with Fabp2, GK, Cpt1a, and Ppara, and negatively correlated with Acsl4 and Pck1 (Fig. 13A). The network diagram showed the same results with a strong correlation between the PPARα signaling pathway and the glycerophospholipid metabolism pathway (Fig. 14A).

Meanwhile, analyses were continued using untargeted metabolomics. Using the PPARα antagonist, GW6471 altered the metabolite composition between groups (Fig. 12A and B). Venn analysis was used to identify the differential proteins shared between the groups, and there were 30 differential proteins shared between the NCD *vs.* the NCD + GW6471 and the HFD *vs.* the HFD + GW6471 groups. There were 56 differential proteins shared with the HFD + *L. reuteri vs.* HFD + *L. reuteri* + GW6471 group (Fig. 12C). In addition, the heat maps of the HFD + *L. reuteri* group and the HFD + *L. reuteri* + GW6471 group showed that the metabolites LPC 19 : 0, LysOPE (20 : 5(5*Z*,8*Z*,11*Z*,14*Z*,17*Z*)/0 : 0), and PG (18 : 1(11*Z*)/20 : 4 (5*Z*.8*Z*,11*Z*,14*Z*)) varied significantly. They all belonged to the glycerol ester metabolic pathway (Fig. 15A). KEGG pathway analysis illustrated, from another perspective, that the differential metabolites clustered in the glycerol ester metabolic pathway (Fig. 15B). Conclusively, the weight loss effect of *L. reuteri* was achieved with the help of the combined action of PPAR and glycerophospholipids metabolism. *L. reuteri* ultimately exerts its weight loss effect by regulating the interaction between PPAR and the glycerophospholipid metabolic pathway (Fig. 16).

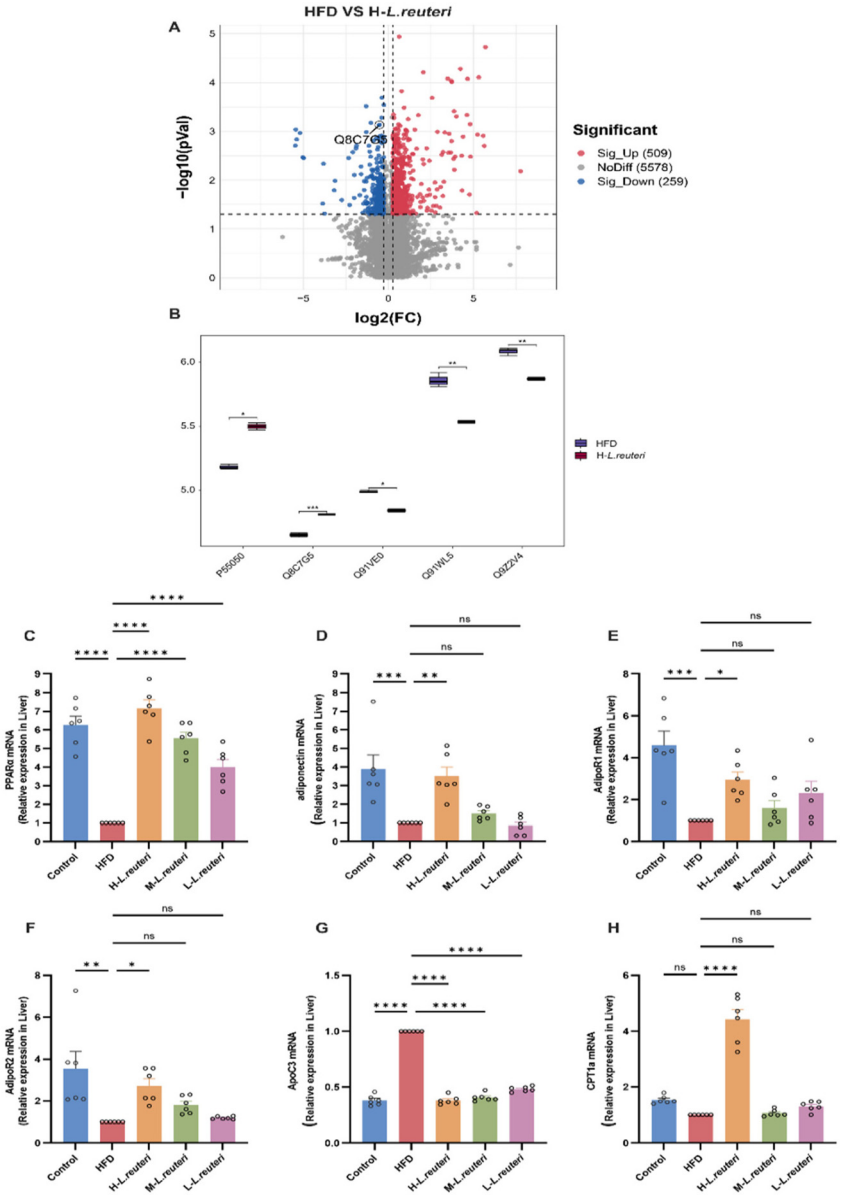

Fig. 9 *L. reuteri* affects the PPARα signalling pathway. (A) Volcano plots of the H-*L. reuteri vs.* the HFD group. (B) Box-line plots of differential proteins in the PPAR signaling pathway (UniProt-gene: Q8C7G5-Apoa5; 09Z2V4-Pckl; Q91WL5-Cyp4a12a; Q91VE0-Slc27a4; P55050-Fabp2). (C–H) Relative expression of PPAR-α, adiponectin, AdipoR1, AdipoR2, ApoC3 and CPT1a in the liver tissue, respectively. Data are expressed as means ± SEM; *$p < 0.05$, **$p < 0.01$ and ***$p < 0.001$.

4. Discussion

L. reuteri, a type of lactic acid bacteria, has been widely used in food and industrial fermentation and healthcare and has been approved by the U.S. Food and Drug Administration (FDA) for safety status.[49,50] Currently, *L. reuteri* has been repeatedly reported by independent research groups to be highly promising in alleviating metabolic syndrome.[13,19] In support of these findings, we also confirmed the ameliorative effect of *L. reuteri* on obesity. We found that *L. reuteri* attenuated weight gain due to a fatty diet, which is similar to the results formerly reported in the literature.[17,51] In general, weight gain leads to alterations in several organs, especially liver fat accumulation, adipose tissue expansion, and imbalance of blood glucose and insulin homeostasis.[52,53] Our study confirms this conclusion that *L. reuteri* effectively reduced fat weight and liver weight and improved glucose tolerance and insulin resistance in obese mice. These outcomes revealed that *L. reuteri* has a mitigating effect on obesity.

Besides, we further explored the influences of *L. reuteri* on lipid accumulation in HFD mice. The lipid quartet includes TC, TG, LDL-C, and HDL-C.[54,55] They are essential markers of lipid accumulation and reflect the state of fat storage and metabolism in the body.[56] Compared with the HFD group, the

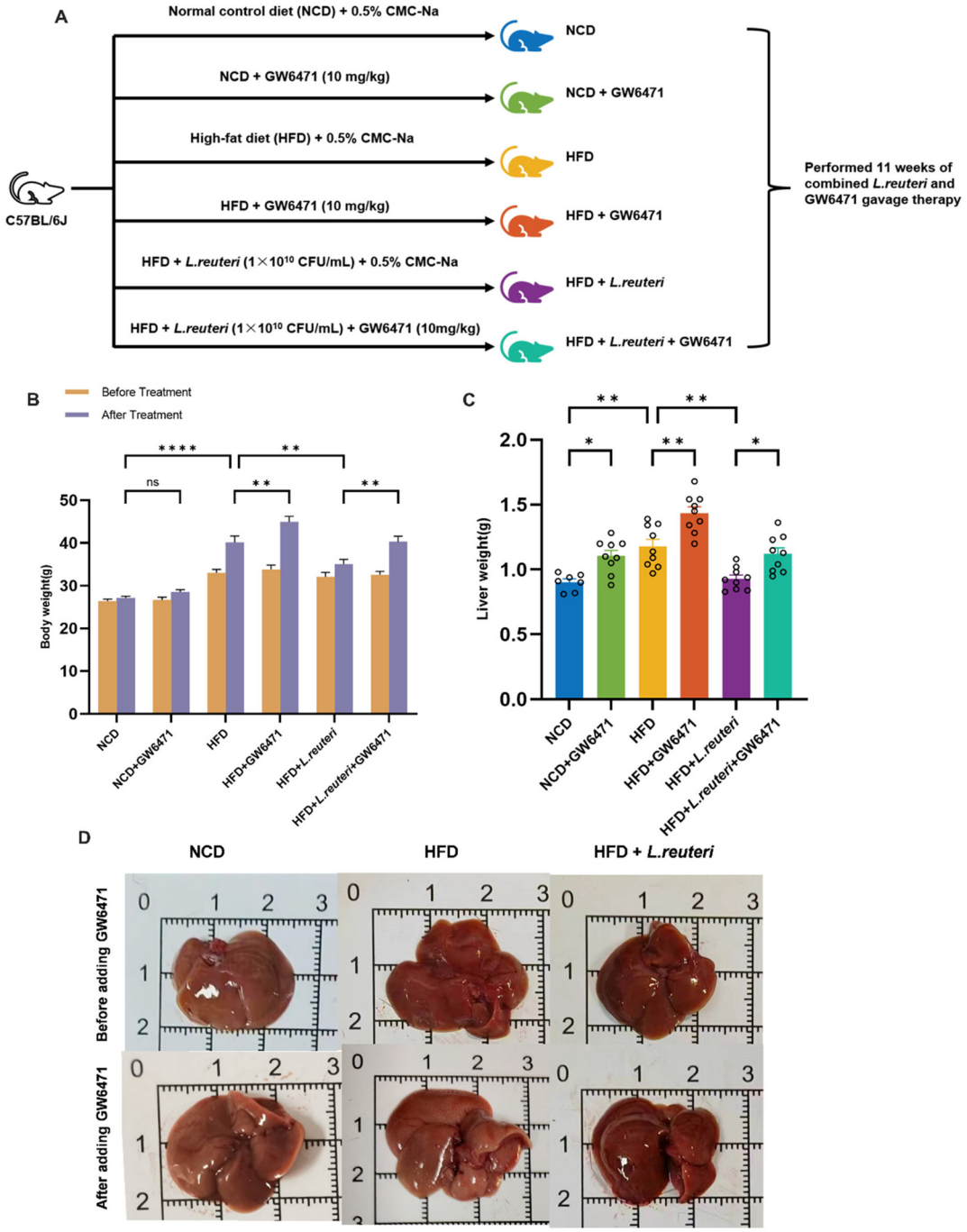

Fig. 10 The PPARα antagonist GW6471 greatly impairs obesity alleviation by *L. reuteri*. (A) Design of the experiments. (B) Changes in the body weight of mice over 11 weeks. (C) Liver weight. (D) Morphological demonstration of the liver. Data are expressed as mean ± SEM. *$p < 0.05$, **$p < 0.01$, ***$p < 0.001$ and ****$p < 0.0001$.

L. reuteri intervention decreased TC, TG, and LDL-C levels and increased HDL-C, similar to the results of Huang *et al.* and Liu *et al.*[57,58] Hepatic inflammation and hepatic steatosis were found to occur in HFD mice as determined by oil red O staining and H&E staining, suggesting that obesity may promote hepatic lipid metabolism disorders, similar to the results previously reported in the literature.[20] In addition, our results showed that the 1×10^{10} CFU mL^{-1} dose of the *L. reuteri* administration group was almost close to the control group, indicating that the high dose of *L. reuteri* had the most significant effect on the improvement in the mice. However, the mechanisms behind these effects remain elusive. Therefore, it

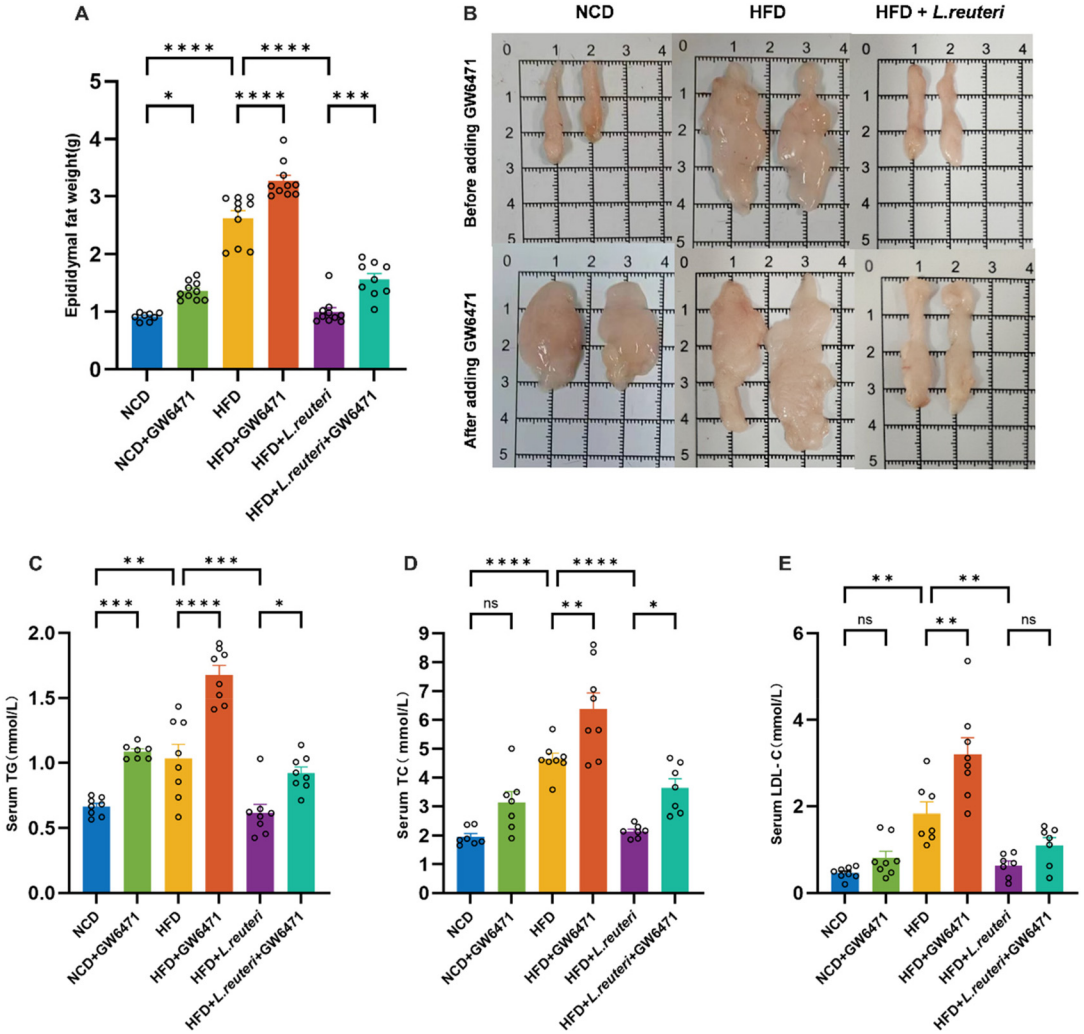

Fig. 11 GW6471 exacerbates lipid deposition in mice. (A) Epididymal fat weight. (B) Demonstration of the epididymal fat morphology. (C) The level of TG in serum. (D) The level of TC in serum. (E) The level of LDL-C in serum. Data are expressed as means ± SEM. *$P < 0.05$, **$P < 0.01$, ***$P < 0.001$ and ****$P < 0.0001$.

is essential to explore the lipid metabolism regulated by *L. reuteri* and to identify host targets associated with obesity.

When fat accumulation in the body increases, the metabolic demand of the liver also increases. Once the metabolic capacity of the liver cells is overloaded, metabolic disorders occur, leading to liver cell injury.[31,59] In the previous part, we judged the ameliorative effect of *L. reuteri* on liver injury in high-fat mice by studying the changes of certain biochemical indexes in liver tissue sections and blood. However, it is not enough to study these alone; a more in-depth investigation is needed into the causes of these changes. Lipid metabolism involves a variety of enzymes and metabolic pathways, which are crucial for maintaining cellular function and energy balance and regulating physiological processes.[24,29,54] Therefore, this study measured the enzymatic activities of several key regulatory enzymes related to fatty acid production: CPT-1, ACC, and FAS in the mouse liver to understand fat accumulation *in vivo*. ACC catalyzes the formation of malonyl monoacyl coenzyme A from acetyl coenzyme A, and the amount of this product controls fatty acid metabolism to a certain extent.[60] It has been reported that high ACC levels in the liver promote the synthesis of triglycerides, which in turn increases the risk of developing hyperlipidemia.[61] In the current experiment, the ACC content in the livers of the H-*L. reuteri* group was appreciably diverged from that of the model group, which means that high-dose feeding can reduce hepatic lipid accumulation in hyperlipidaemic mice. FAS is a multifunctional homodimeric protein, the primary enzyme required for metabolizing carbohydrates into fatty acids.[62] Inhibition of FAS activity irreversibly suppresses endogenous fatty acid synthesis, thereby inhibiting tumor cell proliferation and inducing apoptosis.[63] The FAS content in the livers of all three experimental groups was lower than that of the model group, and all of them were markedly different. CPT-1 acts as a transporter of acetyl groups inside and outside the mitochondrial membrane together with acetyl coenzyme

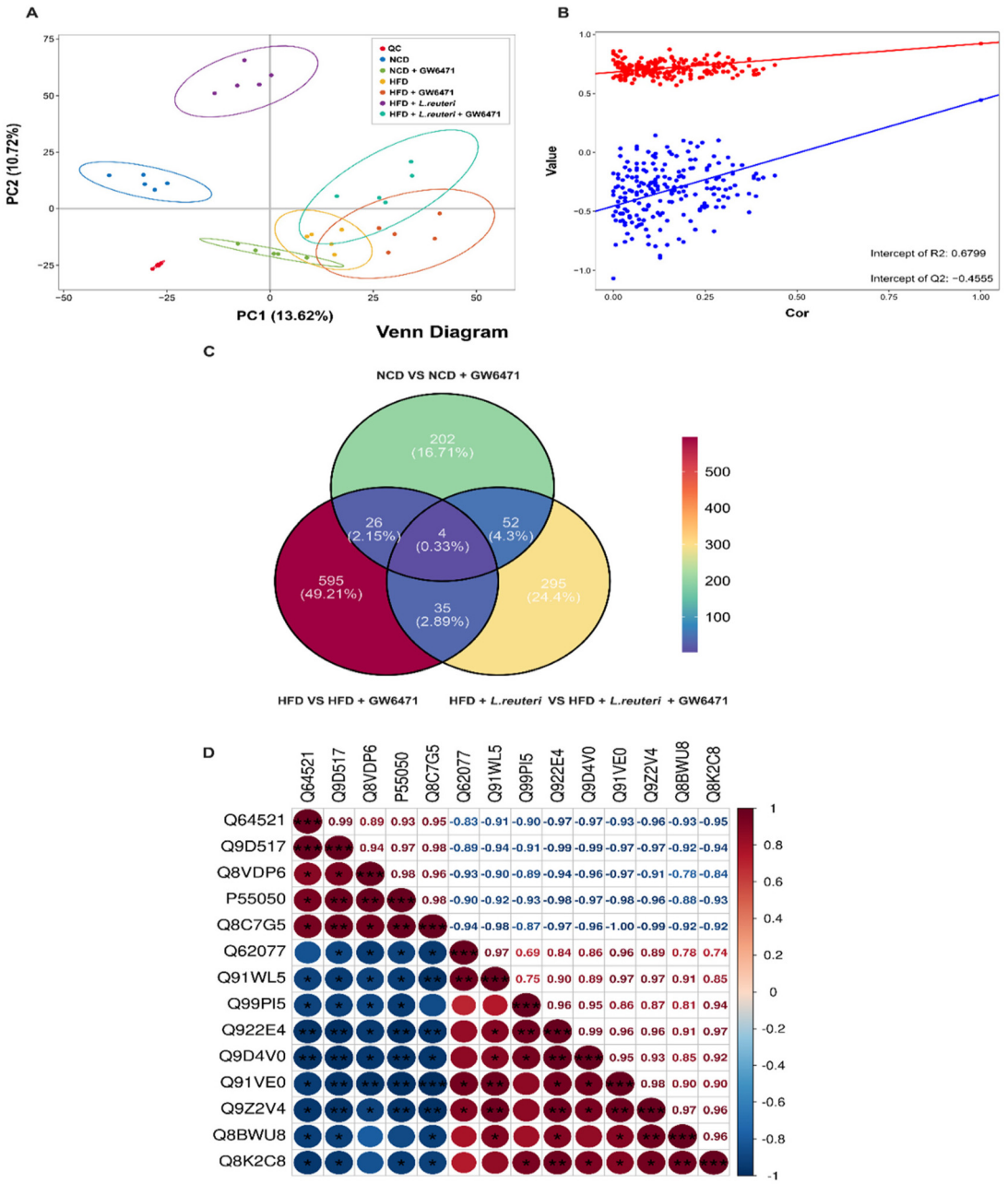

Fig. 12 The PPARα signaling pathway is strongly correlated with the glycerophospholipid metabolic pathway. (A) PLS-DA plots for the six groups. (B) Six group replacement test charts. (C) Differential protein Venn plots for the control, HFD and H-*L. reuteri* groups. (D) Plot of the correlation coefficients of differential proteins between the H-*L. reuteri* and HFD groups.

A.[64,65] The levels of CPT-1 in the livers of all three experimental groups were above those of the control group, with the best results in the high-dose group. These results suggest that *L. reuteri* may reduce lipid accumulation in high-fat mice, and this trend was more pronounced for the 1×10^{10} CFU mL^{-1} dose of *L. reuteri*.

In the first half of the experiment, we examined the influence of *L. reuteri* on fatty acid metabolism in hyperlipidaemic mice. Various associations between fatty acids and body fat have been published. When fatty acids are over-accumulated, free fatty acids can be used as substrates to produce lipotoxic substances (ceramides, diacylglycerols, lysophosphatidylcholine, *etc.*), triggering oxidative stress in the body, which ultimately leads to hepatocellular damage and fibrosis.[66–68] Studying the lipid status of the organism provides a clear understanding of its lipid metabolism. It is an effective way to explore the specific mechanism of the mitigating effect of *L. reuteri* on liver injury in high-fat mice. We observed significant changes in the hepatic metabolite composition after *L. reuteri* intervention, a finding that is consistent with the

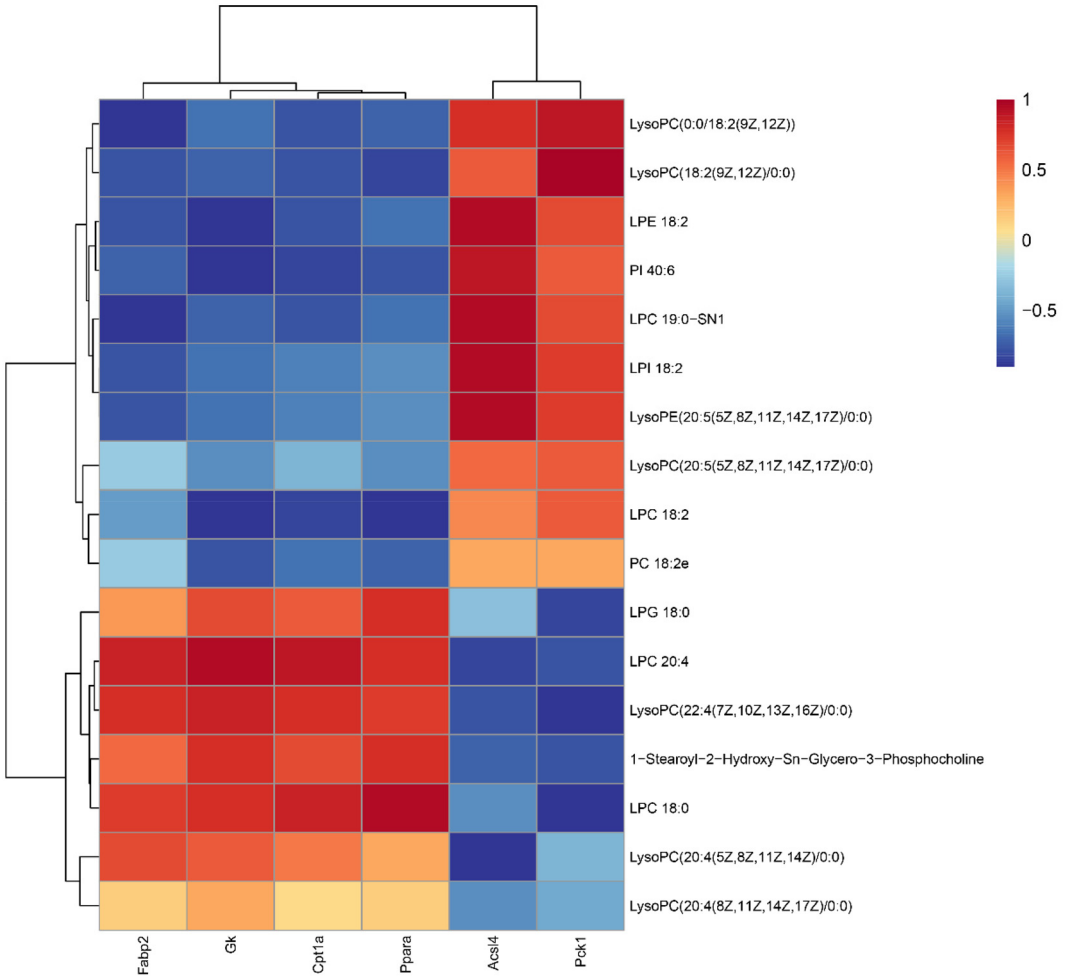

Fig. 13 PPARα signaling pathway is strongly correlated with glycerophospholipid metabolism. (A) Heatmap for the joint analysis of PPARα signaling pathway differential proteins correlating with glycerophospholipid metabolites.

results reported for hydrolyzed guar gum in high-fat model mice.[69] In addition, a previous study showed that rhodopsin ameliorated lipid metabolism disorders by modulating lipidomic profiles in obese mice.[70] In contrast to these observations, we found that administration of *L. reuteri* resulted in significant changes in mouse liver metabolites represented by PC, LysoPC, PG, and LysoPG. Correlation analysis found that these metabolites cluster in the glycerophospholipid metabolic pathway, a branch of the lipid metabolic pathway. The fatty acid groups on glycerophospholipids can be oxidized and decomposed to produce energy for cellular use. In addition, glycerophospholipids can also act as carriers of fatty acids and participate in the transportation and metabolism of fatty acids.[71,72] The findings described above demonstrate that *L. reuteri* alleviates obesity by regulating fatty acid metabolism, which supports the hypothesis that its lipid-lowering effects depend on the regulation of glycerophospholipid metabolic pathways. Therefore, it is reasonable to suspect that *L. reuteri* depends on regulating glycerophospholipid metabolic pathways to exert its lipid-lowering effects.

Next, we further explored the changes in the glycerophospholipid metabolic pathway after *L. reuteri* intervention at the protein level. Unsurprisingly, differential proteins remained significantly enriched in the glycerophospholipid metabolic pathway. The significant changes in the differential protein Apoa5 drew our attention. Studies have shown that *APOA5* may be the gene with the most significant effect on triglycerides and their metabolism.[47] Triglyceride metabolism is closely related to glycerophospholipid metabolism; both have the glycerol molecule as their core structure and intersect during fatty acid synthesis, storage, and transport.[48] A search for PPARα signaling pathway proteins revealed that the differential proteins Apoa5 and Fabp2 were significantly up-regulated, and Cyp4a12a, Pck1, and Slc27a4 were significantly down-regulated in the H-*L. reuteri* group compared to the HFD group. In addition to Apoa5, Fabp2, Cyp4a12a, Pck1 and Slc27a4 were also closely related to metabolic fatty acids. FABP2 binds fatty acids and facilitates fatty acid transport across cell membranes, and participates in fatty acid uptake and metabolism in the small intestine.[73] CYP4A12A is engaged in the long-

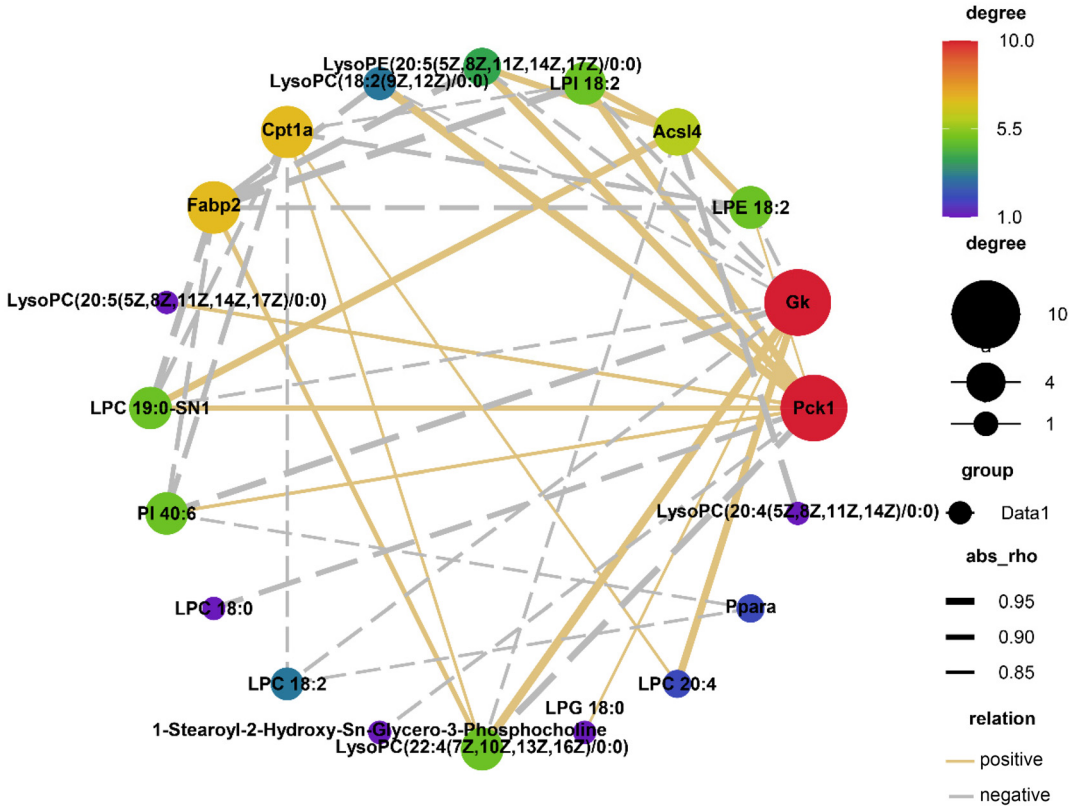

Fig. 14 PPARα signaling pathway is strongly correlated with glycerophospholipid metabolism.(A) Network diagram of the PPARα signaling pathway correlating with glycerophospholipid metabolism.

chain fatty acid synthesis and promotes fatty acid oxidation.[74] Increased activity of PCK1 may affect fatty acid synthesis and storage, which in turn affects lipid metabolism.[75] SLC27A4 can transport exogenous fatty acids into the cell for energy production or conversion to fat storage.[76] The present study also demonstrated at the gene level that activation of PPARα acts on lipid metabolism by affecting adiponectin and its receptors AdipoR1 and AdipoR2, regulating upstream and downstream genes *ApoC3* and *CPT-1* to maintain lipid homeostasis and thus enhancing the activity of PPARα, which ultimately promotes the oxidation of fatty acids. Overall, we conclude that the PPARα pathway is a lynchpin for the ameliorative effects of *L. reuteri* on obesity.

To establish the mechanistic basis underlying the observed lipid reduction, this study delineates that the anti-obesity effect of *L. reuteri* stems from a PPARα-mediated reprogramming of hepatic lipid metabolism. This activation drives a dual metabolic shift: it simultaneously enhances fatty acid β-oxidation and suppresses *de novo* lipogenesis. The upregulation and increased activity of CPT-1, a direct PPARα target, provide functional evidence for the enhanced catabolic disposal of lipids. Concurrently, the suppression of the lipogenic enzymes ACC and FAS curtails new fat synthesis. Critically, the inhibition of ACC exerts a dual effect that extends beyond simply reducing substrate availability for fatty acid synthesis. By alleviating malonyl-CoA's allosteric blockade of CPT-1, ACC inhibition simultaneously relieves a key brake on mitochondrial fatty acid oxidation, creating a synergistic 'push–pull' mechanism that efficiently redirects metabolic flux toward oxidation rather than storage.[60,62] Indeed, the malonyl-CoA/CPT-1 axis serves as a key metabolic checkpoint, ensuring that fatty acid oxidation is actively suppressed when synthesis is ongoing and reciprocally derepressed when synthetic demand decreases.[64,65] Our findings show that *L. reuteri* effectively exploits this endogenous regulatory circuit to reprogram hepatic lipid metabolism. This shift, together with the upregulation of Apoa5—a key regulator of triglyceride-rich lipoprotein metabolism—adds another dimension to the observed lipid-lowering effect by improving lipid export.[47,48] Collectively, these coordinated changes in specific metabolic pathways—enhanced fatty acid oxidation, suppressed *de novo* lipogenesis, and improved lipid export—conclusively explain the reduction in hepatic lipid deposition observed in *L. reuteri*-treated mice.

It is important to note that direct measurement of PPARα protein abundance (*e.g.*, *via* immunoblotting) was not conducted in the current study. Nevertheless, our experimental strategy incorporated multiple orthogonal approaches that collectively yield compelling evidence at the protein and functional levels. Specifically, DIA-based quantitative proteomics enabled the unbiased identification of protein-level alterations within the PPARα signaling network, including the upregulation of Apoa5 and Fabp2 and the downregulation of Cyp4a12a,

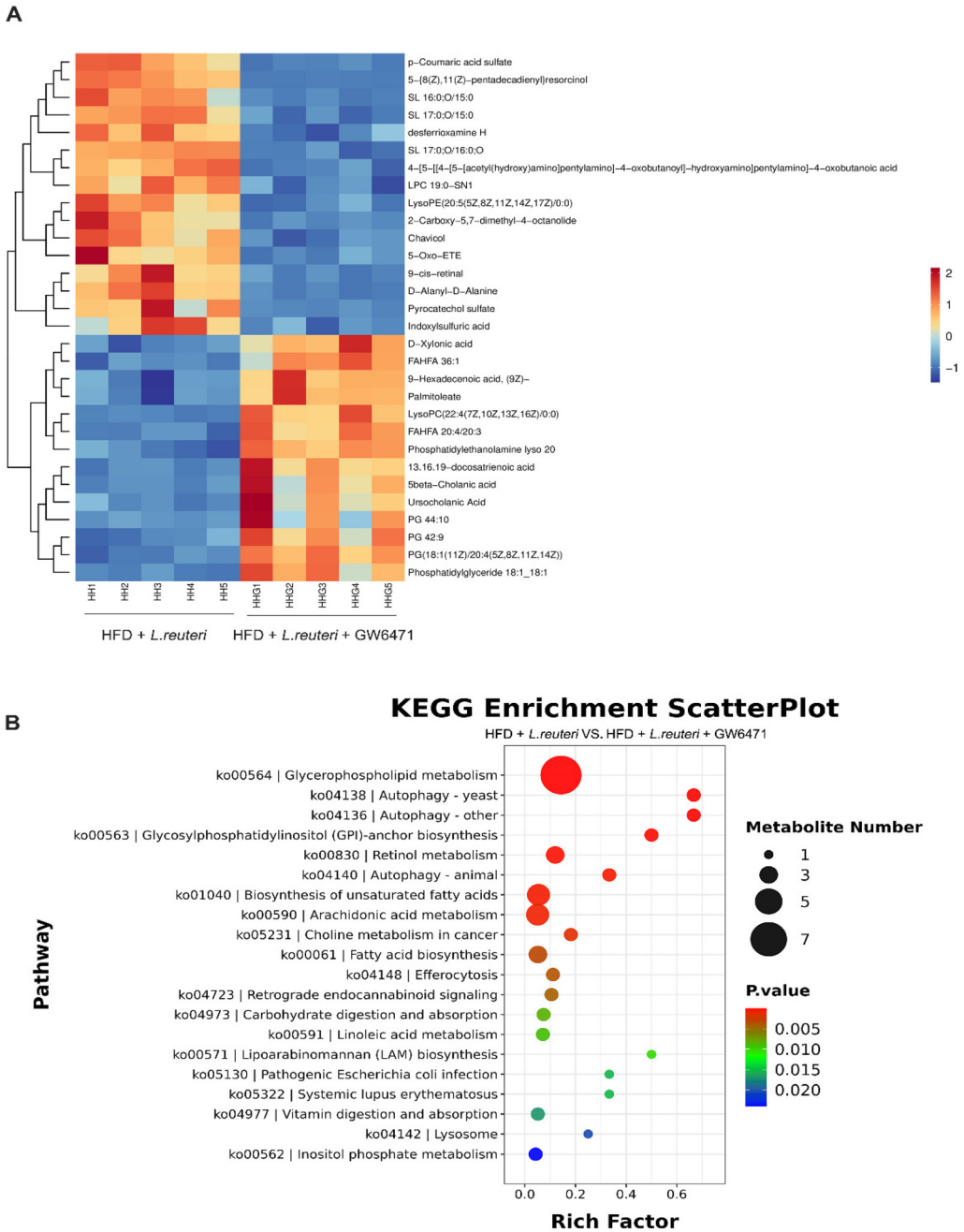

Fig. 15 The PPARα signaling pathway synergizes with glycerophospholipid metabolism to exert lipid-lowering effects. (A) Heat maps of non-targeted metabolites in the HFD + *L. reuteri* and HFD + *L. reuteri* + GW6471 groups. (B) Bubble plots of non-targeted metabolites in the HFD + *L. reuteri* and HFD + *L. reuteri* + GW6471 groups.

Pck1, and Slc27a4 (Fig. 9B). These findings show that the key components of the PPARα pathway were modulated at the protein level in response to *L. reuteri* intervention. Additionally, ELISA was employed to quantify the protein levels of critical downstream effectors—CPT-1, FAS, and ACC (Fig. 3A–C). The increased activity of CPT-1, along with the reduced levels of ACC and FAS, aligns with the established functions of these enzymes in promoting fatty acid oxidation while suppressing *de novo* lipogenesis.[60,62,64,65] Beyond these protein-centric measurements, the pharmacological blockade of PPARα with GW6471 abrogated the beneficial metabolic outcomes associated with *L. reuteri* treatment (Fig. 10 and 11), providing the strongest functional evidence that this pathway is not merely correlated but causally required. Collectively, these complementary lines of evidence—spanning quantitative proteomics, targeted protein assays, and antagonist-based validation—form a cohesive and robust foundation supporting the engagement of the PPARα pathway.

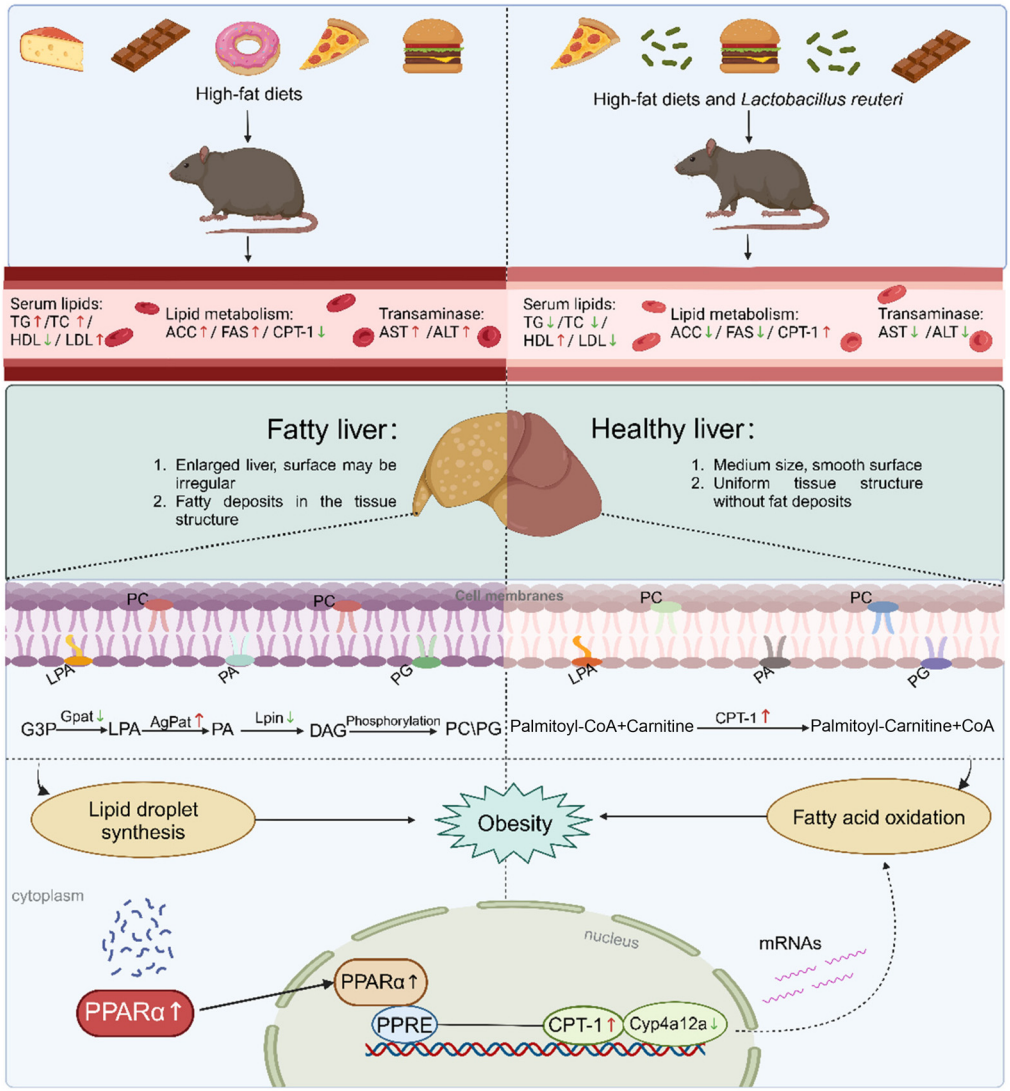

Fig. 16 Mechanisms of *L. reuteri* alleviating high-fat diet-induced obesity in mice.

Regarding the mode of action, it is highly improbable that *L. reuteri* acts by directly binding to hepatic PPARα. Instead, the available evidence supports an indirect mechanism involving multiple layers of host-mediated signaling. Our metabolomic analysis revealed that *L. reuteri* intervention profoundly reshapes the hepatic glycerophospholipid metabolome, leading to significant alterations in lysophosphatidylcholine (LPC) and phosphatidylcholine (PC) species (Fig. 4–6). These metabolites have been reported to serve as endogenous PPARα ligands or signaling mediators,[71,72] suggesting that *L. reuteri* may act indirectly by modulating the availability of such bioactive lipids. Second, gut-derived signals likely contribute to this regulatory network. Short-chain fatty acids (SCFAs) produced by microbial fermentation, as well as secondary bile acids generated through gut microbiota metabolism, can reach the liver *via* the portal vein and have been shown to modulate PPARα activity.[23,45] Collectively, these findings indicate that *L. reuteri* does not directly engage PPARα but rather establishes a host-mediated metabolic and signaling milieu—originating from both remodeled hepatic phospholipid metabolism and altered gut microbial output—that permissively activates the central PPARα regulatory hub in the liver.

In summary, *L. reuteri* ameliorates obesity-associated hepatic steatosis by activating the PPARα signaling pathway, which in turn transcriptionally coordinates a metabolic shift favoring lipid oxidation over storage.[29,64] This work advances the understanding from phenomenological association to a defined mechanistic framework involving specific metabolic pathways.[20,45] Looking forward, further characterization of this gut–liver axis should focus on identifying the precise bacterial and host-derived effector molecules that initiate the signaling cascade, employing tissue-specific models to dissect cellular autonomy and validating the translational relevance of these mechanisms in human studies.[19,23,59] Addressing these questions will solidify the mechanistic foundation and explore the therapeutic potential of targeting this microbiome–host metabolic interface.[13,49]

While this study establishes a clear link between *L. reuteri* supplementation and the amelioration of HFD-induced obesity *via* the PPARα–glycerophospholipid axis, certain methodological considerations are acknowledged to contextualize the findings and guide future work. First, the experimental design focused on the therapeutic context of obesity, and therefore did not include a group receiving *L. reuteri* under a normal chow diet (NCD). This design choice prioritizes the investigation of *L. reuteri* as an intervention against established metabolic dysfunction, which is its most relevant potential application. The observed effects—reversal of weight gain, dyslipidemia, and hepatic steatosis—are specifically tied to counteracting HFD-induced pathology. The literature on probiotic interventions often employs similar therapeutic models to elucidate mechanisms within a disease state, as the primary goal is to restore homeostasis rather than to characterize baseline effects in healthy subjects. Second, the mechanistic insights are derived from integrated *in vivo* analyses, including antagonist studies which provide strong pharmacological causality for the PPARα pathway. Although *in vitro* models using hepatocytes would offer a reductionist platform to dissect direct cellular effects, our *in vivo* approach captures the essential host–microbe interactions within the gut–liver axis, which are central to probiotic action and cannot be fully recapitulated in isolated cell systems. Future studies incorporating both NCD + *L. reuteri* controls and *in vitro* hepatocyte models treated with *L. reuteri*-conditioned media or key metabolites will be invaluable to delineate the direct microbial signals from the systemic physiological responses and to confirm the cell-autonomous role of the identified PPARα mechanism.

Author contributions

Aibei Zhu: conceptualization, writing – original draft, investigation, data curation and methodology. Wenjuan Shen: conceptualization, data curation, formal analysis, investigation, methodology, software, and writing – original draft. Bibi Zainab: software and investigation. Xiaohu Luo: supervision and project administration. Xiping Wu: formal analysis and investigation. Yanan Liu: writing – review & editing, supervision, project administration, and funding acquisition.

Conflicts of interest

The authors confirm that there are no conflicts of interest associated with this study.

Ethics approval and consent to participate

All animal experimental procedures were carried out under the Guidelines for the Welfare and Ethical Use of Laboratory Animals developed by the National Standardization Administration of China and approved by the Animal Ethics Committee of the Medical School of Ningbo University (Zhejiang, China) (approval number: 11805).

Data availability

The raw data of non-targeted metabolomics reported in this study have been deposited in the MetaboLights database (https://www.ebi.ac.uk/metabolights/MTBLS12293).

Acknowledgements

The present study was supported by the Open Project Program of the State Key Laboratory of Food Science and Resources, Jiangnan University (No. SKLF-KF-202306) and the Open Project Program of the Key Laboratory of Agricultural Product Quality Evaluation and Nutrition and Health, Ministry of Agriculture and Rural Affairs, Zhejiang University (No. ZJU-APQHLAB-2405).

References

1 Z. M. Younossi, M. Kalligeros and L. Henry, Epidemiology of metabolic dysfunction-associated steatotic liver disease, *Clin. Mol. Hepatol.*, 2024, **31**, 532–550.
2 G. Marcelin, A. L. M. Silveira, L. B. Martins, A. V. Ferreira and K. Clément, Deciphering the cellular interplays underlying obesity-induced adipose tissue fibrosis, *J. Clin. Invest.*, 2019, **129**, 4032–4040.
3 M. E. Piché, A. Tchernof and J. P. Després, Obesity phenotypes, diabetes, and cardiovascular diseases, *Circ. Res.*, 2020, **126**, 1477–1500.
4 C. M. Perdomo, R. V. Cohen, P. Sumithran, K. Clément and G. Frühbeck, Contemporary medical, device, and surgical therapies for obesity in adults, *Lancet*, 2023, **401**, 1116–1130.
5 O. Brown, H. McGowan, J. Gierula, M. Drozd, M. Kearney, E. Levelt, S. Wheatcroft, M. Conning-Rowland, M. Bailey, K. Griffin, L. Roberts, K. Paradine, R. Ajjan, S. Straw, M. Giannoudi and R. Cubbon, The relationship between diabetes, obesity and cardiovascular disease phenotypes: a uk biobank cohort study, *Heart*, 2023, **109**, 232–234.
6 S. Pouwels, M. P. Buise, P. Twardowski, P. S. Stepaniak and M. Proczko, Obesity surgery and anesthesiology risks: A review of key concepts and related physiology, *Obes. Surg.*, 2019, **29**, 2670–2677.
7 J. Fink, G. Seifert, M. Blüher, S. Fichtner-Feigl and G. Marjanovic, Obesity surgery-weight loss, metabolic changes, oncological effects, and follow-up, *Dtsch. Aerztebl. Int.*, 2022, **119**, 70–80.
8 B. Dubern, [Genetics and epigenetics of obesity: keys to understand], *Rev. Prat.*, 2019, **69**, 1016–1019.
9 V. M. Jackson, D. M. Breen, J. P. Fortin, A. Liou, J. B. Kuzmiski, A. K. Loomis, *et al.*, Latest approaches for

the treatment of obesity, *Expert Opin. Drug Discov.*, 2015, **10**, 825–839.
10 S. K. Kim, R. B. Guevarra, Y. T. Kim, J. Kwon, H. Kim, J. H. Cho, *et al.*, Role of Probiotics in Human Gut Microbiome-Associated Diseases, *J. Microbiol. Biotechnol.*, 2019, **29**, 1335–1340.
11 J. Suez, N. Zmora, E. Segal and E. Elinav, The pros, cons, and many unknowns of probiotics, *Nat. Med.*, 2019, **25**, 716–729.
12 T. L. Bedada, T. K. Feto, K. S. Awoke, A. D. Garedew, F. T. Yifat and D. J. Birri, Probiotics for cancer alternative prevention and treatment, *Biomed. Pharmacother.*, 2020, **129**, 110409.
13 T. L. Montgomery, K. Eckstrom, K. H. Lile, S. Caldwell, E. R. Heney, K. G. Lahue, *et al.*, *Lactobacillus reuteri* tryptophan metabolism promotes host susceptibility to CNS autoimmunity, *Microbiome*, 2022, **10**, 198.
14 M. Hu, F. He, Y. Guo, L. Mo and X. Zhu, *Lactobacillus reuteri* biofilms inhibit pathogens and regulate microbiota in vitro fecal fermentation, *J. Agric. Food Chem.*, 2022, **70**, 11935–11943.
15 J. Wang, H. Zhang, H. Yuan, S. Chen, Y. Yu, X. Zhang, *et al.*, Prophylactic Supplementation with *Lactobacillus Reuteri*, or Its Metabolite GABA Protects Against Acute Ischemic Cardiac Injury, *Adv. Sci.*, 2024, **11**, 2400–2229.
16 N. Li, L. Niu, Y. Liu, Y. Wang, X. Su, C. Xu, *et al.*, Taking SCFAs produced by *Lactobacillus reuteri* orally reshapes gut microbiota and elicits antitumor responses, *J. Nanobiotechnol.*, 2024, **22**, 147.
17 K. M. Yang, J. S. Kim, H. S. Kim, Y. Y. Kim, J. K. Oh, H. W. Jung, *et al.*, *Lactobacillus reuteri* AN417 cell-free culture supernatant as a novel antibacterial agent targeting oral pathogenic bacteria, *Sci. Rep.*, 2021, **11**, 17164.
18 W. Liu, W. Shen, P. Weng, Z. Wu and Y. Liu, Novel chlorella pyrenoidosa peptides attenuate weight gain, insulin resistance, and lipid levels in mice fed a high-fat diet, *J. Funct. Foods*, 2024, **112**, 105908.
19 Z. Lin, J. Wu, J. Wang, C. L. Levesque and X. Ma, Dietary *Lactobacillus reuteri* prevent from inflammation mediated apoptosis of liver *via* improving intestinal microbiota and bile acid metabolism, *Food Chem.*, 2023, **404**, 134643.
20 Y. Liu, X. Zhong, S. Lin, H. Xu, X. Liang, Y. Wang, *et al.*, *Limosilactobacillus reuteri* and caffeoylquinic acid synergistically promote adipose browning and ameliorate obesity-associated disorders, *Microbiome*, 2022, **10**, 2663.
21 F. Seebacher, A. Zeigerer, N. Kory and N. Krahmer, Hepatic lipid droplet homeostasis and fatty liver disease, *Semin. Cell Dev. Biol.*, 2020, **108**, 72–81.
22 J. Chen, Y. Zhou, Z. Liu, Y. Lu, Y. Jiang, K. Cao, *et al.*, Hepatic glycogenesis antagonizes lipogenesis by blocking S1P via UDPG, *Science*, 2024, **383**, eadi3332.
23 J. Kuang, J. Wang, Y. Li, M. Li, M. Zhao, K. Ge, *et al.*, Hyodeoxycholic acid alleviates non-alcoholic fatty liver disease through modulating the gut-liver axis, *Cell Metab.*, 2023, **35**, 1752–1766.
24 S. Jeon and R. Carr, Alcohol effects on hepatic lipid metabolism, *J. Lipid Res.*, 2020, **61**, 470–479.
25 T. Balla, N. Sengupta and Y. J. Kim, Lipid synthesis and transport are coupled to regulate membrane lipid dynamics in the endoplasmic reticulum, *Biochim. Biophys. Acta, Mol. Cell Biol. Lipids*, 2020, **1865**, 158461.
26 N. Bougarne, B. Weyers, S. J. Desmet, J. Deckers, D. W. Ray, B. Staels, *et al.*, Molecular Actions of PPARα in Lipid Metabolism and Inflammation, *Endocr. Rev.*, 2018, **39**, 760–802.
27 Y. Lin, R. Liu, Y. Huang, Z. Yang, J. Xian, J. Huang, *et al.*, Reactivation of PPARα alleviates myocardial lipid accumulation and cardiac dysfunction by improving fatty acid β-oxidation in Dsg2-deficient arrhythmogenic cardiomyopathy, *Acta Pharm. Sin. B*, 2023, **13**, 192–203.
28 I. Barbagallo, L. Vanella, M. T. Cambria, D. Tibullo, J. Godos, L. Guarnaccia, *et al.*, Silibinin Regulates Lipid Metabolism and Differentiation in Functional Human Adipocytes, *Front. Pharmacol.*, 2016, **6**, 698.
29 O. O. Badmus, S. A. Hillhouse, C. D. Anderson, T. D. Hinds and D. E. Stec, Molecular mechanisms of metabolic associated fatty liver disease (MAFLD): Functional analysis of lipid metabolism pathways, *Clin. Sci.*, 2022, **136**, 1347–1366.
30 T. Balla, N. Sengupta and Y. J. Kim, Lipid synthesis and transport are coupled to regulate membrane lipid dynamics in the endoplasmic reticulum, *Biochim. Biophys. Acta, Mol. Cell Biol. Lipids*, 2020, **1865**, 158629.
31 V. Petrenko, F. Sinturel, H. Riezman and C. Dibner, Lipid metabolism around the body clocks, *Prog. Lipid Res.*, 2023, **91**, 101235.
32 T. Le Roy, E. M. de Hase, M. Van Hul, A. Paquot, R. Pelicaen, M. Régnier, *et al.*, Dysosmobacter welbionis is a newly isolated human commensal bacterium preventing diet-induced obesity and metabolic disorders in mice, *Gut*, 2022, **71**, 534–543.
33 C. He, K. Wang, J. Xia, D. Qian, J. Guo, L. Zhong, *et al.*, Natural exosomes-like nanoparticles in mung bean sprouts possesses anti-diabetic effects via activation of PI3K/Akt/GLUT4/GSK-3β signaling pathway, *J. Nanobiotechnol.*, 2023, **21**, 317.
34 L. Ding, Q. Yang, E. Zhang, Y. Wang, S. Sun, Y. Yang, *et al.*, Notoginsenoside Ft1 acts as a TGR5 agonist but FXR antagonist to alleviate high fat diet-induced obesity and insulin resistance in mice, *Acta Pharm. Sin. B*, 2021, **11**, 1541–1554.
35 A. Lama, C. Pirozzi, I. Severi, M. G. Morgese, M. Senzacqua, C. Annunziata, *et al.*, Palmitoylethanolamide dampens neuroinflammation and anxiety-like behavior in obese mice, *Brain, Behav., Immun.*, 2022, **102**, 110–123.
36 X. Feng, M. Du, S. Li, Y. Zhang, J. Ding, J. Wang, *et al.*, Hydroxysafflor yellow a regulates lymphangiogenesis and inflammation via the inhibition of PI3K on regulating AKT/mTOR and NF-κB pathway in macrophages to reduce atherosclerosis in ApoE$^{-/-}$ mice, *Phytomedicine*, 2023, **112**, 154684.
37 J. Ding, M. Xu, W. Du, Z. Fang, H. Xu, J. Liu, *et al.*, Myeloid-specific blockade of Notch signaling ameliorates nonalco-

holic fatty liver disease in mice, *Int. J. Biol. Sci.*, 2023, **19**, 1941–1954.
38 M. Tian, F. Hao, X. Jin, X. Sun, Y. Jiang, Y. Wang, *et al.*, ACLY ubiquitination by CUL3-KLHL25 induces the reprogramming of fatty acid metabolism to facilitate iTreg differentiation, *eLife*, 2021, **10**, 72689.
39 S. Wang, Y. Lin, L. Gao, Z. Yang, J. Lin, S. Ren, *et al.*, PPAR-γ integrates obesity and adipocyte clock through epigenetic regulation of Bmal1, *Theranostics*, 2022, **12**, 1589–1606.
40 K. Barathikannan, R. Chelliah, S. Vijayalakshmi, F. K. Ofosu, S. J. Yeon, D. S. Lee, *et al.*, Untargeted metabolomics and gut microbiota modulation study of fermented brown rice for obesity, *ACS Omega*, 2024, **9**, 37636–37649.
41 Y. Liu, M. Zhao, Y. Yu, J. Liu, W. Liu, R. Yao, *et al.*, Extracellular cold-inducible RNA- binding protein mediated neuroinflammation and neuronal apoptosis after traumatic brain injury, *Burns Trauma*, 2024, **12**, 313.
42 Z. Wang, X. Wang, L. Fu, S. Xu, X. Wang, Q. Liao, *et al.*, Shengmai San formula alleviates high-fat diet-induced obesity in mice through gut microbiota-derived bile acid promotion of M2 macrophage polarization and thermogenesis, *Phytomedicine*, 2024, **133**, 155938.
43 E. K. Sims, A. L. J. Carr, R. A. Oram and L. A. DiMeglio, Evans Molina C. 100 years of insulin: celebrating the past, present and future of diabetes therapy, *Nat. Med.*, 2021, **27**, 1154–1164.
44 S. H. Lee and K. H. Yoon, A century of progress in diabetes care with insulin: A history of innovations and foundation for the future, *Diabetes Metab. J.*, 2021, **45**, 629–640.
45 C. Zhang, R. Fang, X. Lu, Y. Zhang, M. Yang, Y. Su, *et al.*, *Lactobacillus reuteri*, J1 prevents obesity by altering the gut microbiota and regulating bile acid metabolism in obese mice, *Food Funct.*, 2022, **13**, 6688–6701.
46 H. Xiao, X. Sun, Z. Lin, Y. Yang, M. Zhang, Z. Xu, *et al.*, Gentiopicroside targets PAQR3 to activate the PI3K/AKT signaling pathway and ameliorate disordered glucose and lipid metabolism, *Acta Pharm. Sin. B*, 2022, **12**, 2887–2904.
47 M. Guardiola and J. Ribalta, Update on APOA5 genetics: Toward a better understanding of its physiological impact, *Curr. Atheroscler. Rep.*, 2017, **19**, 30.
48 A. Giammanco, R. Spina, A. B. Cefalù and M. Averna, APOC III: A gatekeeper in controlling triglyceride metabolism, *Curr. Atheroscler. Rep.*, 2023, **25**, 67–76.
49 A. Saviano, M. Brigida, A. Migneco, G. Gunawardena, C. Zanza, M. Candelli, *et al.*, *Lactobacillus Reuteri* DSM 17938 (*Limosilactobacillus reuteri*) in diarrhea and constipation: Two sides of the same coin?, *Medicina*, 2021, **57**(7), 643.
50 A. P. dos R. B. Zermiani, A. L. P. P. de P. Soares, B. L. da S. G. de Moura, E. R. A. Miguel, L. D. G. Lopes, N. de C. S. Santana, *et al.*, Evidence of *Lactobacillus reuteri* to reduce colic in breastfed babies: Systematic review and meta-analysis, *Complement Ther Med.*, 2021, **63**, 102781.
51 Q. Cen, Y. Cui, J. Feng, L. Zhu, J. Wei, L. Wang, C. Chang, R. Pang, J. Wang and A. Zhang, *Limosilactobacillus reuteri* DSM17938 Attenuates Neuroinflammatory Responses After Spinal Cord Injury by Modulating Tryptophan Metabolism, *Probiotics Antimicrob. Proteins*, 2025, **18**(1), 1–19.
52 U. Galicia-Garcia, A. Benito-Vicente, S. Jebari, A. Larrea-Sebal, H. Siddiqi, K. B. Uribe, *et al.*, Pathophysiology of Type 2 Diabetes Mellitus, *Int. J. Mol. Sci.*, 2023, **24**, 13883.
53 M. C. Petersen, D. F. Vatner and G. I. Shulman, Regulation of hepatic glucose metabolism in health and disease, *Nat. Rev. Endocrinol.*, 2017, **13**, 572–587.
54 C. H. Cho, S. Patel and P. Rajbhandari, Adipose tissue lipid metabolism: lipolysis, *Curr. Opin. Genet. Dev.*, 2023, **83**, 102114.
55 A. Yang and J. McNabb-Baltar, Hypertriglyceridemia and acute pancreatitis, *Pancreatology*, 2020, **20**, 795–800.
56 L. Da Dalt, A. G. Cabodevilla, I. J. Goldberg and G. D. Norata, Cardiac lipid metabolism, mitochondrial function, and heart failure, *Cardiovasc. Res.*, 2023, **119**, 1905–1914.
57 Q. Liu, Z. Zhang, P. Ji, J. Liu, B. Chen, E. Mingyao, *et al.*, Ginseng polysaccharide components attenuate obesity and liver lipid accumulation by regulating fecal microbiota and hepatic lysine degradation, *Int. J. Biol. Macromol.*, 2024, **269**, 131872.
58 Y. Huang, J. Hu, Q. Xia, M. Tang, Y. Wang, G. Wang, *et al.*, Amelioration of obesity and inflammation by polysaccharide from unripe fruits of raspberry via gut microbiota regulation, *Int. J. Biol. Macromol.*, 2024, **261**, 129825.
59 H. Gao, Z. Jin, G. Bandyopadhyay, G. Wang, D. Zhang, K. C. E. Rocha, *et al.*, Aberrant iron distribution via hepatocyte-stellate cell axis drives liver lipogenesis and fibrosis, *Cell Metab.*, 2022, **34**, 1201–1213.
60 L. Gao, Z. Xu, Z. Huang, Y. Tang, D. Yang, J. Huang, *et al.*, CPI-613 rewires lipid metabolism to enhance pancreatic cancer apoptosis via the AMPK-ACC signaling, *J. Exp. Clin. Cancer Res.*, 2020, **39**, 327.
61 M. Liu, Z. Zhang, Y. Chen, T. Feng, Q. Zhou and X. Tian, Circadian clock and lipid metabolism disorders: A potential therapeutic strategy for cancer, *Front. Endocrinol.*, 2023, **14**, 483–490.
62 I. K. Cerk, L. Wechselberger and M. Oberer, Adipose triglyceride lipase regulation: An overview, *Curr. Protein Pept. Sci.*, 2017, **19**, 123.
63 A. K. Sharma, R. Khandelwal and C. Wolfrum, Futile lipid cycling: from biochemistry to physiology, *Nat. Metab.*, 2024, **6**, 808–824.
64 Z. Shan, H. Zhang, C. He, Y. An, Y. Huang, W. Fu, *et al.*, High-protein mulberry leaves improve glucose and lipid metabolism via activation of the PI3K/Akt/PPARα/CPT-1 pathway, *Int. J. Mol. Sci.*, 2024, **25**, 8726.
65 I. R. Schlaepfer and M. Joshi, CPT1A-mediated fat oxidation, mechanisms, and therapeutic potential, *Endocrinology*, 2020, **161**, b046.
66 E. Currie, A. Schulze, R. Zechner, T. C. Walther and R. V. Jr. Farese, Cellular fatty acid metabolism and cancer, *Cell Metab.*, 2013, **18**, 153–161.
67 J. M. Weiss, E. M. Palmieri, M. Gonzalez-Cotto, I. A. Bettencourt, E. L. Megill, N. W. Snyder, *et al.*, Itaconic

acid underpins hepatocyte lipid metabolism in non-alcoholic fatty liver disease in male mice, *Nat. Metab.*, 2023, **5**, 981–995.

68 Y. Poitelon, A. M. Kopec and S. Belin, Myelin Fat Facts: An Overview of Lipids and Fatty Acid Metabolism, *Cells*, 2020, **9**, 3633.

69 X. Fu, Z. Liu, R. Li, J. Yin, H. Sun, C. Zhu, *et al.*, Amelioration of hydrolyzed guar gum on high-fat diet-induced obesity: Integrated hepatic transcriptome and metabolome, *Carbohydr. Polym.*, 2022, **297**, 120051.

70 L. Cheng, S. Zhang, F. Shang, Y. Ning, Z. Huang, R. He, *et al.*, Emodin Improves Glucose and Lipid Metabolism Disorders in Obese Mice via Activating Brown Adipose Tissue and Inducing Browning of White Adipose Tissue, *Front. Endocrinol.*, 2021, **12**, 618037.

71 M. R. Gonzalez-Baro and R. A. Coleman, Mitochondrial acyltransferases and glycerophospholipid metabolism, *Biochim. Biophys. Acta, Mol. Cell Biol. Lipids*, 2017, **1862**, 49–55.

72 W. J. Valentine, T. Hashidate-Yoshida, S. Yamamoto and H. Shindou, Biosynthetic Enzymes of Membrane Glycerophospholipid Diversity as Therapeutic Targets for Drug Development, *Adv. Exp. Med. Biol.*, 2020, **1274**, 5–27.

73 E. Maculewicz, A. Leońska-Duniec, A. Mastalerz, E. Szarska, A. Garbacz, T. Lepionka, *et al.*, The influence of FTO, FABP2, LEP, LEPR, and MC4R genes on obesity parameters in physically active caucasian men, *Int. J. Environ. Res. Public Health*, 2022, **19**, 12428.

74 K. J. R. Hoyer-Allo, M. R. Späth, S. Brodesser, Y. Zhu, J. Binz-Lotter, M. Höhne, *et al.*, Caloric restriction reduces the pro-inflammatory eicosanoid 20-hydroxyeicosatetraenoic acid to protect from acute kidney injury, *Kidney Int.*, 2022, **102**, 560–576.

75 Q. Ye, Y. Liu, G. Zhang, H. Deng, X. Wang, L. Tuo, *et al.*, Deficiency of gluconeogenic enzyme PCK1 promotes metabolic-associated fatty liver disease through PI3K/AKT/PDGF axis activation in male mice, *Nat. Commun.*, 2023, **14**, 6290.

76 C. Shen, Z. Pan, W. Xie, J. Zhao, D. Miao, L. Zhao, *et al.*, Hepatocyte-specific SLC27A4 deletion ameliorates nonalcoholic fatty liver disease in mice via suppression of phosphatidylcholine-mediated PXR activation, *Metabolism.*, 2025, **162**, 156054.

